An experimental study on the stability behaviour of curved CFRP panel under axial compression load

Shiv Krishan Chandra

A Thesis Submitted to
Indian Institute of Technology Hyderabad
In Partial Fulfilment of the Requirements for
The Degree of Master of Technology

भारतीय प्रौद्योगिकी संस्थान हैदराबाद
Indian Institute of Technology Hyderabad

Department of Department of Mechanical and Aerospace Engineering

June 2018

Declaration

I declare that this written submission represents my ideas in my own words, and where ideas or words of others have been included, I have adequately cited and referenced the original sources. I also declare that I have adhered to all principles of academic honesty and integrity and have not misrepresented or fabricated or falsified any idea/data/fact/source in my submission. I understand that any violation of the above will be a cause for disciplinary action by the Institute and can also evoke penal action from the sources that have thus not been properly cited, or from whom proper permission has not been taken when needed.
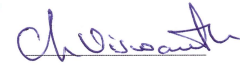
(Signature)

Shiv Krishan Chandra
(Student Name)

ME16MTECH11015
(Roll No.)

Approval Sheet

This thesis entitled **An experimental study on the stability behaviour of curved CFRP panel under axial compression load** by Shiv Krishan Chandra is approved for the degree of Master of Technology from IIT Hyderabad.

(Dr. Viswanath Chinthapenta, Assistant professor) Examiner,
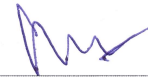Department of Mechanical and Aerospace Engineering,
IIT Hyderabad.

(Dr. Syed Nizamuddin Khaderi, Assistant professor) Examiner,
Department of Mechanical and Aerospace Engineering,
IIT Hyderabad.

(Dr. M. Ramji, Associate professor) Adviser,
Department of Mechanical and Aerospace Engineering,
IIT Hyderabad.

(Dr. Gangadharan Raju, Assistant professor) Co-Adviser,
Department of Mechanical and Aerospace Engineering,
IIT Hyderabad.

(Dr. S. Suriya Prakash, Associate professor) Chairman,
Department of Civil Engineering,
IIT Hyderabad.

Acknowledgements

Dedication

Dedicated to
God, Dear Parents, and Teachers

Abstract

Aerospace cylindrical composite structures are thin-walled by nature and their structural design is primarily governed by its stability behaviour. In this work, the buckling and post buckling behaviour of shallow curved CFRP panels under axial compression is investigated by digital image correlation (DIC) systems. A novel attempt is made using multiple DIC systems to capture the displacement and strain fields over the flat regions of the curved panel in the pre-buckling, buckling and post-buckling regimes. Curved composite panels of various stacking sequences such as uni-directional $[0]_8$, cross-ply$[0/90]_4$, quasi-isotropic$[45/90/-45/0]_s$ are fabricated using hand layup and vacuum bagging technique. Special loading fixtures are designed to apply uniform compression load on the curved edges of the panel. Experiments are conducted to study the effect of free and simply supported plate boundary conditions being applied on the longitudinal edges. A finite element modeling(FEM) of the curved CFRP panel using continuum shell element in ABAQUS is carried out to study the buckling and post-buckling behavior. The actual imperfection of the fabricated curved panel is measured using coordinate measuring machine (CMM). Further, the measured imperfections are given as input for performing Riks post-buckling analysis and the results are compared with experimental observation for validation.

Contents

List of Figures

List of Tables

Nomenclature

B	Width of panel
CFRP	Carbon Fibre Reinforced Polymer
CMM	Coordinate measuring Machine
DIC	Digital Image Correlations
FEA	Finite Element Method
L	Length of the panel
R	Radius of curvature
UD	Unidirectional
s	Symmetric
t	Thickness of panel
ρ	Density of resin material

Chapter 1

Introduction and Literature review

1.1 Introduction

Composite materials are widely used in aerospace, civil, naval, and marine engineering fields due to their specific properties such as strength and stiffness with respect to weight ratio compared to conventional metals. The components of the automobile such as roof, hoods, mufflers, interior panels of cars etc. made of composite. Use of composite materials in automobile industries shown in Fig. 1.1(a).[1] and aerospace industries shown in figure 1.1(b)[2].
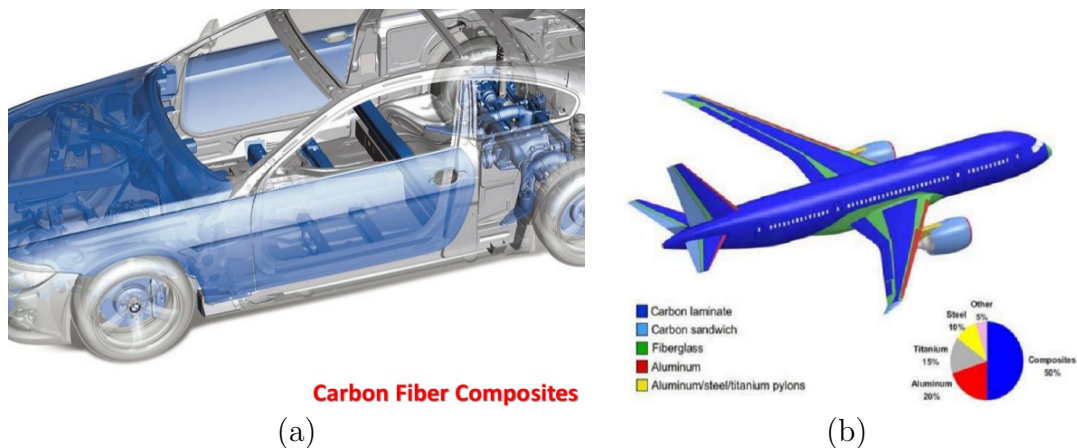
Figure 1.1: (a) Use of composite materials in automobile industries and (b) Use of composite materials in aerospace industries.

Composite materials are stronger than conventional materials, a thin structure can have carried the high load. So the industries have moved its research focus on the to lightweight composite panels and shells and integrated into the commercial structure. But the cost of the composite materials is high. To optimize the cost, the volume of the composite structure should be less and it can be done by an appropriate reduction in the thickness. But when structures are thin and subjected to an axial compression load, stability of the structure is an important design criterion based on the

---

[1]Source:-https://www.slideshare.net/ratnachatterjee/advanced-future-applications-of-composite-fibres-in-the-automotive-industry.

[2]Source:-https://image.slidesharecdn.com

strength. Because it will buckle before the material failure of the structure and stop its functionality. For more than forty years researchers have tried to relate the behavior of thin walled structures in the buckling and post-buckling region, calculating the initial buckling load and predict the load displacement behaviour and load-carring capacity.

In simple words, buckling is out of plane deformation of the specimen or it may be defined as the loss of stability of object due to their geometric effects rather than material failure. It may because of material failure if the consequent deformations are not restrained. Most of the structures are working within the elastic limit range. Elastic limit is a point up-to structure return to the original position upon removal of the applied load. Permanent deformations occur if elastic limit range crossed as matrix cracking occurs in composite.

Most of the aerospace industries and others structures are curved in nature. Some example of the curved structures as shown in Fig. 1.2[3].

Figure 1.2: Example of curved composite structure

Buckling load of a panel largely depends upon the imperfections present in composite panel. Any such imperfection would critically affect the panel and may eventually lead to catastrophic failure of the structure. There are different types of imperfection in composite materials such as geometric imperfections, materials non-homogenities and load eccentricity imperfections. Geometric imperfection refers to deviation of the midplane of the panel from its original shape when it is not subjected any load i.e. no stress. These imperfections can be created by the residual stress when the panel was fabricated or it may simply be due to the limitations in the accuracy of the manufacturing process. And it is impossible to avoid the imperfections while fabricating the specimen. Method for calculating the imperfection is given by the Thornburgh 2006 [1].These imperfection has substantial bad effect on the buckling and post buckling behaviour of the curved composite structures. Out of these imperfections, geometric imperfection plays the major role. For example- geomentric imperfection, with maximum amplitude to panel thickness ratio of 0.5, was found to reduce buckling load of compiste cylinders by 40%. [2]

But there are few researchers who worked on the curved panels. buckling of curved panels may be due to bifurcation point described by Khot 1982 [3] which requires geometric non-linear analysis. Buckling response due to thermal and mechanical loading studied by the Breivik 1998 [4] and Breivik 1998 has also shown buckling response for different boundary condition.

---

[3]Source: http://www.automateddynamics.com

1.2 Literature review

Khot et.al [3] worked on a numerical and experimental investigation of the buckling behavior of composite panels. They gave initial buckling behavior of circular composite panel. In this paper, researchers team used clamped boundary conditions along the curved edge of the specimen and unsupported and supported boundary conditions along the flat edge of the specimen under uni-axial compression load. The author validated his experimental result with a numerical prediction based upon an energy-based, finite difference and computer program CLAPP. He suggested that isotopic, orthotropic and anisotropic plates and panels can lose their load carrying capacity through a loss of stability in two ways: either bifurcation buckling point or an unacceptable degradation of their stiffness that results in excessive displacement without appearing of a bifurcation point[5, 6]. The author used eight-layers graphite-epoxy material laminate to form the $[0/90]_{2s}$. The overall thickness of the specimen is close to 0.038 inch and radius of curvature is 12 inch (304.8 mm). The length and width of the specimen is 16 inch and 8 inch respectively. The imperfection of the specimen is measured by the mechanical device which consists of the dial indicator. For unsupported boundary conditions, initial stiffness of panel agree quite well with the numerical result and for the simply supported boundary condition, the results were much better than first experiments.

K.D.Kim [7] studied on the buckling behaviour of the composite panel using finite element method. In this paper, formulation of the non-geometric non-linear composite shell element based upon the updated Lagrangian method is considered to buckling response of the shell. Eight node element with six degrees of freedom were selected,since it can capture small strain and large deformation with finite rotation during analysis. Non dimensionless buckling loads Nb^2/E_2h^3 compared with Noor's,khadier and Librescu. Noor results were based upon the 3D elasticity solution using finite difference method whereas Khadier and Librescu solution based upon a theory of incorporation with higher order shear deformation theory. Two examples were taken into account for the validation of the analysis. First, a thick cross-ply [0/90] composite plate with three, five and nine layers were taken. Properties used in this paper are

$$E_1 = 40E_2, \quad G_{12} = G_{23} = 0.6E_2, \quad \nu_{12} = 0.25.$$

Secondly,a symmetric cross-ply panel $[0/90]_s$ with same properties were considered. Simply boundaries condition with axial compression load used. The result obtain from this formulation was good with first order shear deformation theory but effect of higher-order theory were not good.

Breivik 1998 studied the buckling and post-buckling behaviour of the curved composite panel, due to thermal and mechanical loading, where they considered three different layup sequences ($[45/-45/0/90]_s$,$[45/-45/90]_s$, $[45/-45/0]_s$) with clamped boundaries condition, along the curved edges, and sliding or fixed simply supported boundary condition, along the straight edge of the panel. Mechanical loading is applied by the same deformation at every endpoint with neglecting temperature variation and thermal loading is applied by the increasing the same temperature at spatial location with restricted deformation along end edge. Linear buckling analysis of axially compressed curved panel reported by the koiter. Linear Donnell-type buckling equation was solved. The membrane analysis allowed only the axial stress resultant to exist, while other two stress resultant were assumed to be zero. STAGS finite element used Riks method to obtain the solution along the unstable loading paths. 411 type element used for modelling the panel. These elements are

quadrilateral faceted shell elements. Each node is allowed six degree of freedom which consists of three rotational and three displacements. The author observed that the loss of the load capacity due to the post-buckling ranges upto 50% for the $[45/90]_{2s}$ which is lamented with sliding simple support for a softening of the response relation as in case with thermally loaded $[45/0/90]_s$ it is laminated with fixed simple support. Buckling load for clamped/fixed simply supported is greater the buckling load for clamped/sliding simply supported case.

M. Lakshmi Aparna [8] studied in the fabrication of continuous GFRP composites using vacuum bag moulding process. In this paper, step by step procedure for the fabrication of unidirectional glass fiber reinforced polymer composite specimen using Vacuum bagging the technique has been proposed. In which Unidirectional E-Glass fiber with an aerial density of 430GSM was used as reinforcement and Epofine-230 + Finehard-951 as resin & hardener respectively for the matrix material.

F.A.Featherston [9, 10] studied on the effect of the geometric imperfection on the buckling and post-buckling behavior of the composite panels.Present of imperfections such as geometric, load eccentricity, and material non-homogeneity have considerable effect on the stability of thin-walled composite panels.[2] I twas found that out of this imperfection, geometric imperfection has a major contribution[11]. If the ratio of geometric imperfection to the thickness of the panel is 0.5 ,buckling load reduced to 35%. As we know that geometric imperfection is highly responsible for reduction in the buckling load. Generally used techniques have been based upon the knock down factor which is applied to the eigen mode which is obtained from the eigen buckling analysis of the perfect structure. Arbocz [12] has studied on a series of the shape and size imperfection data which have been obtained using a probe moving over the structure's surface to get the outer surface points.A method for importing of the imperfection in commercial finite element software has developed. Five specimens with a different radius of curvature used for validated the method. Digital image correlation data used for FEA modelling. Two types of mesh were used. First, the regular mesh which consists of the three-dimensional array (horizontal pixel, vertical pixel and coordinate). In this mesh, elements are uniformly spaced. Matlab used for obtaining the 3D array data form digital image correlation data. Second, smart mesh in which element was adjusted according to the radius of curvature of the panel. For higher curvature, a number of elements are high and vice-versa.

Thornburgh [1] studied on imperfection and measurement of panels using a coordinate measuring machine. In this paper, Brown and Sharpe global image CMM used for the measuring the coordinate of the specimen and an automation software, PC-DMIS version 3.7 used to control the CMM. MeasPanel software which written by the NASA to act as a graphical user interface (GUI) and provide an easy method for controlling the data input and output of the PC-DMIS software. The measuring of the panels with CMM machine requires three different processes. (1) panel definition, (2) measurement and (3) post-processing. Panel definition and post-processing are done by the MeasPanel software and measurement are done by the PC-DMIS software. Thickness data is obtained by subtracting opposing scan points on the inner and outer surfaces.

1.3   Objective

A review of literature shows that a lot of work has been done on buckling and post buckling analysis of laminated flat composite plates either by experimental , analytical or numerical based method

(FEM) like ABQUS, STAGS or ANSYS. However, very little work exists on the post-buckling analysis of curved composite plates. Hence the present study was taken up.

The objective of this thesis is to experimentally investigate the buckling and post-buckling response of curved CFRP panel under axial compression and validate it with the numerical results derived from FEM based methods. In order to investigate the buckling and post-buckling response of the specimen, a finite element model of curved composite panel made and numerical analysis has been carried out with the finite element commercial software Abaqus-CAE 2017 and the experiments were carried out with the Digital Image Correlation (DIC) technique. For this work, three different sequences (UD ($[0]_8$),cross-ply ($[0/90]_4$),quasi-isotropic ($[45/-45/90/0]_s$) of curved panels were fabricated by the infusion method. The major scopes of the present investigation are:

- To study the buckling and post-buckling response of curved CFRP panels under axial compression load.

- Use of co-ordinate measuring machine (CMM) for measuring the initial geometric imperfection of the specimens.

- Use of 3D DIC technique for capturing the buckling and post-buckling response of the test panels

- Validation of experimental results with FEA simulations.

- To import the initial geometric imperfection into the FEA simulations.

1.4   Problem definition

The symmetric laminated and curved panels considered in this study are shown in Fig. 1.3.
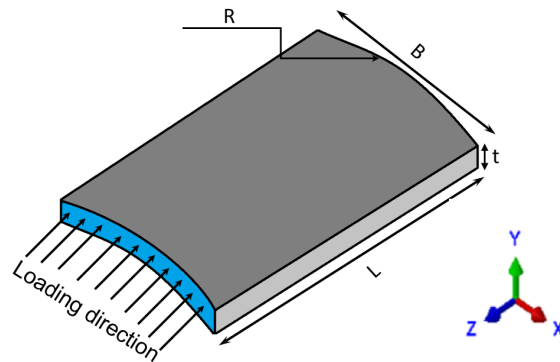
Figure 1.3: Schematic diagram of curved panel

The panels are subjected to axial compressional load along the curved edge, another side of the panel is subjected to simply supported boundary conditions. The stacking sequence details of panels are shown in Table 1.1. Fiber orientations are shown in Fig. 1.4.
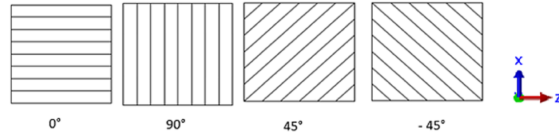
Figure 1.4: fiber orientation angle

Table 1.1: Stacking sequence details of panels

Details	Stacking sequence	No. of layers	Layer Thickness
UD	$[0]_8$	8	0.225 mm
Cross ply	$[0/90]_4$	8	0.225 mm
Quasi layup	$[45/-45/90/0]_s$	8	0.225 mm

1.5 Thesis layout

This section discusses about the layout of the thesis.

Chapter 1 Gives the brief introduction about the composite materail and curved panels along with the literature review and objective of the present study.

Chapter 2 Explains about the fabrication method of the curved CFRP panel along with the imperfection.

Chapter 3 Explains about the experimental studies of curved CFRP panel under axial compressive load.

Chapter 4 Explains the finite element analysis on the buckling and post-post buckling behavior of the curved CFRP panels.

Chapter 5 Covers the results obtained from experimental as well as finite element analysis.

Chapter 6 Contains the conclusion of the present work.

Chapter 7 Contains brief introduction of the future works.

Appendix A Explains about mesh with initial geometry imperfection.

Chapter 2

Fabrication of curved CFRP panel

2.1   Introduction

The objective of the present study is to carry out an experimental studies on the stability behavior of curved composite panel under axial compression load. a standard procedure for fabricating the curved CFRP panels required for doing the experiments. Vacuum infusion method is used for fabricating the panels. Three panels were fabricated which has different stacking sequence. End block were manufactured with epoxy resin (LY- 556) and hardener (HY-951) for supporting the loading condition at the curved edge. This chapter described the vacuum infusion method for fabricating the curved specimens. It also contains the fabrication method for the end block.

2.2   Details of test specimen

Geometric dimensions of curved CFRP panels used in present study is shown in Fig. 2.1. Stacking sequence of the layup is shown in Table 1.1.
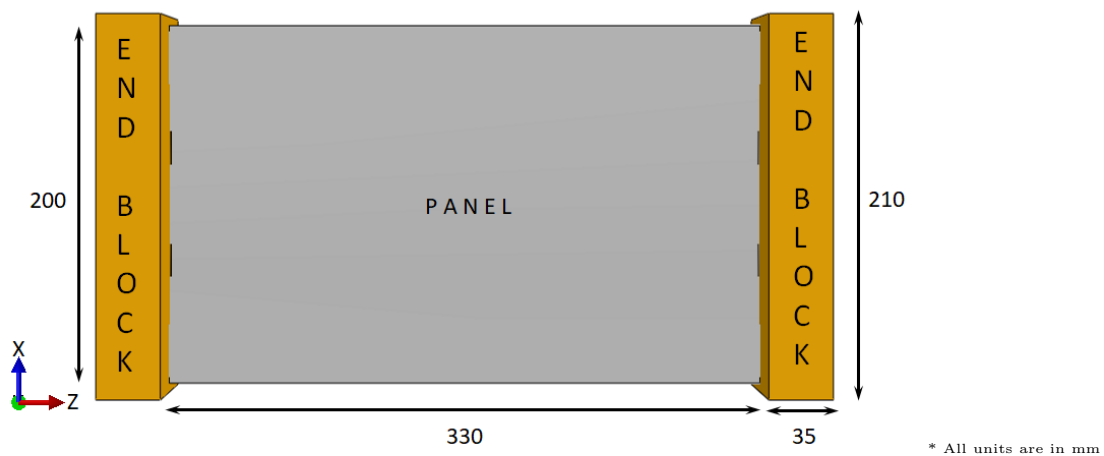
Figure 2.1: Dimensions of the panel (a) Front view (b) Top view

2.3 Fabrication specimen

Three different layup of panels were fabricated during the present study in central workshop IIT Hyderabad. The curved panel was fabricated by vacuum infusion method.

2.3.1 Materials required for fabrication

Materials used for fabricating the specimen are following and shown in Fig. 2.2.

1.UD carbon fibre	4.Epoxy resin	7.Hardener	10.Green mesh
2.acrylic sheet	5.Peel ply	8.Catch pot	11.Spiral tube
3.Vacuum pump	6.Poly cover	9.Sealant tape	12.Acetone
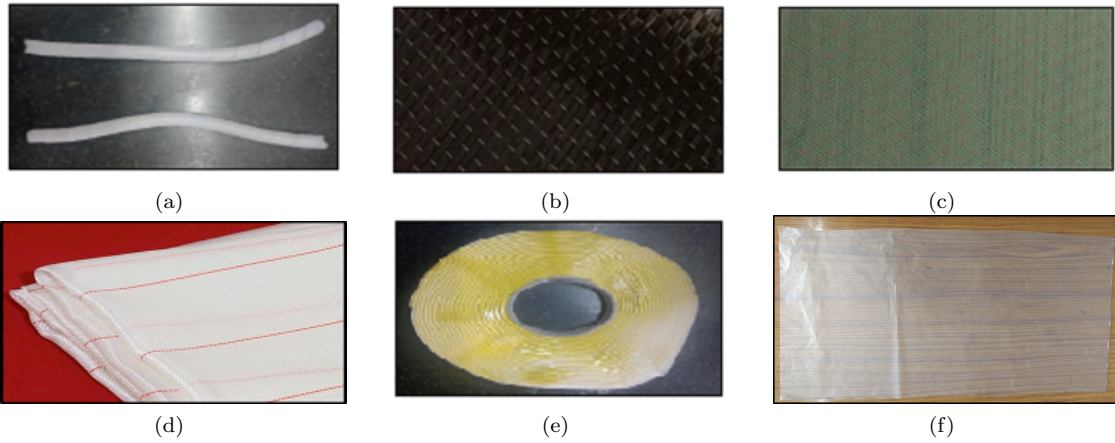
Figure 2.2: Material used for fabricating the panel (a) Spiral tube (b) UD carbon fibre (c) Green mesh (d)Peel ply (e) Sealant tape (f) Perforated sheet

2.3.2 Matrix material

The epoxy resin (Araldite®CY-230)and hardener (Aradur- HY-951) are mixed in the ratio of 10:1 by weight. Weight of resin calculated by Eq. 2.1,

$$w = V\rho, \tag{2.1}$$

where,

w = weight of the resin,

V = volume of the specimen

ρ = density of resin.

The total weight of the matrix material used is 400 gm. So considering the mixing ratio, 360 gm of epoxy resin (Araldite®CY-230) and 40 gm of hardener (Aradur HY951) is taken. The weight taken of matrix material is two times the weight of carbon fibre sheet. This is because if we use exact weights of the resin-hardener mixture, it is not sufficient to wet all the fabric sheets because

some of it gets wasted during spreading, in the infusion tube, flange and catch pot etc. Resin and hardener are mixed and stirred for about 10-12 minute with the help of a mixing scoop to release the dissolved gasses.

2.3.3 Procedure

- First of all, the unidirectional carbon fibre sheet 200 gsm are cut from the carbon fibre bundle. For fabricating eight layers of laminated panel, eight fibre sheets are cut. The dimensions of the carbon fibre sheet are the 420mm long and 220mm wide. Here 20mm tolerance provided in both aspects (length and width).

- Now, the acrylic sheet is fixed on the wooden block has 774 mm radius curvature. This curvature od wooden block is obtained by machining a wooden block (shown in Fig.2.3). The thickness of the acrylic sheet is 5 mm.

- To put the carbon fibre on the acrylic sheet, a rectangular area is marked with the help of a marker. Afterwards, all the layers of carbon fibre sheet are kept on it.

- Now, peel ply is kept upon the fibre sheet.
  Peel Ply - A peel ply is a layer of porous fabric used in the lay-up of a composite material that vents the excess resin and prevents the bagging material from sticking to the carbon fibre sheets. The peel ply is removed after curing of the resin.

- After putting the peel ply, the perforated sheet is kept upon peel ply.
  Perforated sheet - Perforated sheet is pierced with a uniform hole pattern which allows the resin to flow uniformly over the fibre sheets. It can be used in conjugation with release fabric. It helps to hold the resin in the laminate.

- The green mesh sheet is attached over the perforated sheet. Two spiral tubes are fixed on the two opposite sides of the assembly.
  Green mesh- It helps in uniform distribution of the matrix material over the fibre sheet.

- Now, the whole assembly is covered using bagging sheet, and sides are tightly packed using sealant tape, to avoid any air leakage during vacuum bagging.
  Bagging sheet -Bagging sheet forms an airtight envelope around the laminate. It is a transparent in nature and allows easy inspection of the laminate as it cures. Low-temperature nylon vacuum bagging film is used in the fabrication.

- Now, the flange is placed at the bottom and top of the assembly. Flange consists of an infusion tube which is connected to the pot, consists of a matrix material, on one side and catch a pot of vacuum pump on the other side. Here, infusion tube is used for backflow of the excess resin towards the catch pot.

- Vacuum of -700 mm of Hg is applied inside the assembly using the vacuum pump. For some duration, the whole assembly is checked for any air leakage.

- If there is no leakage, a constant vacuum of -500 mm of Hg is applied for 24 hours. In this duration, matrix material from the pot goes slowly inside the assembly and spreads uniformly over the entire length and width of the assembly.
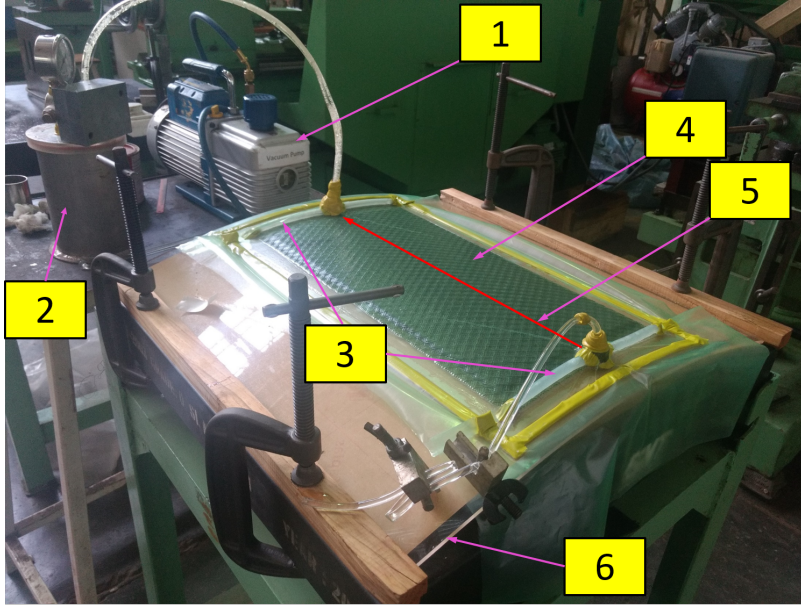
Figure 2.3: Fabrication setup for curved panel (1) vacuum pump (2) catch pot (3) spiral tube (4) poly bag (5) flow direction of resign (6) acrylic sheet

- After curing, the specimen is removed from the assembly.

- Further, machining is done on the specimen for the desired size.

2.3.4 End block Fabrication

End block is fabricated by the mixing of epoxy resin (LY- 556) and hardener (HY-951) in 10 : 1 ratio of weight. The size of end clock is 210 mm length, 60 mm width and 35 mm thickness and 10 mm of shrinkage allowance provided to each side of the mould. Mould setup for end block is shown in Fig. 2.4(a). The mixture is poured into a rectangular mould and kept it for solidification for twenty-four hours. For fixing the end block on the panel, two grooves of 774 radii is cut in the rectangular block. One is 2 mm width throughout the thickness and another one is 6 mm with up to 30 mm of the thickness of the block. The end block fixing setup is shown in Fig. 2.4(b).

After the potting the end block and machining the panel i.e. final specimen is shown in Fig. 2.5.

2.4 Imperfection measurement using Co-ordinate measuring machine (CMM)

CMM is a device for measuring the geometrical characteristics of the specimen. It works on air bell principle. TANGRAM software used for calculation and represent the result in excel file and .IGES file format. CFRP material shrinkage after the solidification so for measuring the average radius and thickness of the panel CMM machine used. 2 mm diameter probe is used for measuring the surface. Firstly, calibration is done with A 0 and B 0 position of the probe tool for measuring the radius of the panel and A 90 and B 90 as well as A 90 and B −90 positions required for measuring the thickness of the panel. Calibration setup is shown in Fig. 2.6
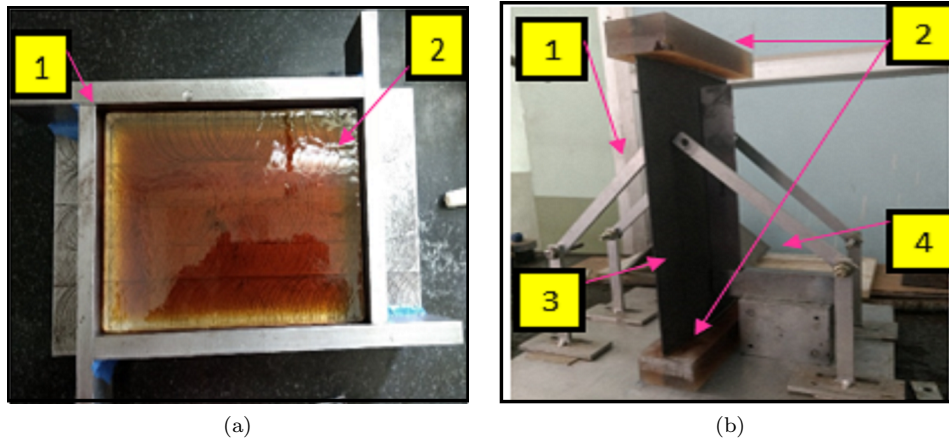
Figure 2.4: (a)Mould setup for end block (1) rectangular mould (2) mixture of resin and hardener (b)End block potting setup (1) holding arms (2) end block (3) curved panel (4) long set square

Figure 2.5: Finished panel

After the calibration, the local coordinate has generated on the one surface of the panel which is in Cartesian co-ordinate. One point is set as a reference point on the panel. For measuring the radius and thickness, 30 curves generated on each surface at 10 mm distance along the length and 2 mm distance along the width.

for measuring the each curve three steps are requried.

- Starting point of the curve.

- A point along which probe will move i.e. it gives the direction to the probe.

- End point of the measuring curve.

These data stored in Tangram software which gives output as an excel file. Setup for measuring the imperfection is shown in Fig. 2.7. After the panel has been scanned, the measured data used for calculating the radius and thickness. Thickness variation data is obtained by the subtracting the
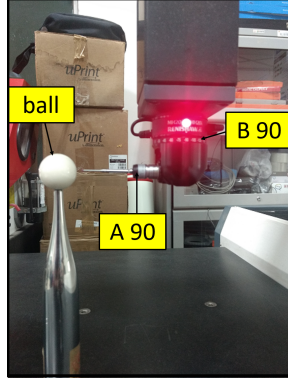
Figure 2.6: Calibration at A 90 and B 90 Position for measurement on CMM

(a)   (b)
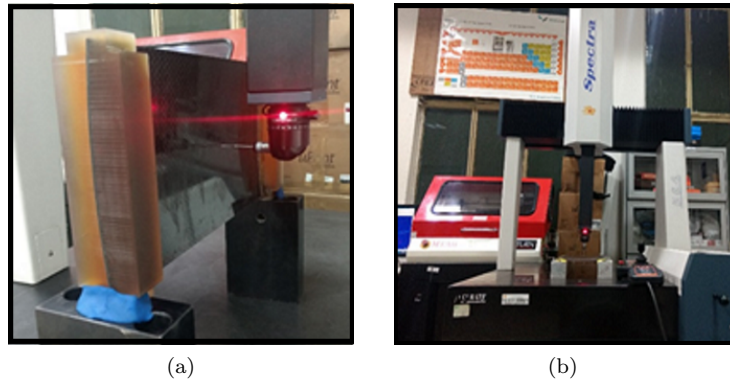
Figure 2.7: CMM setup for measuring the imperfection (a) Set up for thickness measurement (b) Set up for thickness measurement

opposing point on the inner surface and outer surface and divided by the two. For radius calculation, iges file has imported in the solid works software. By joining all the points, the radius of a panel has calculated. The radius of the panel has different at 30 different locations as shown in Figs. 2.8(a),2.9(a) and 2.10(a). And location where points measured in shown in Fig. 2.11.So for doing the numerical analysis, the average value has been considered and shown in Table 2.1.

Table 2.1: Imperfection data obtain from CMM

laminate	Thickness (mm)			Radius (mm)		
	Max.	Min.	Avg.	Max.	Min.	Avg.
Quasi-isotropic $[45/-45/90/0]_s$	1.87	1.67	1.77	760	740	750
Cross-ply $[0/90]_4$	1.85	1.65	1.81	763	737	750
UD $[0]_8$	1.84	1.70	1.78	770	730	750

* All units are in mm.
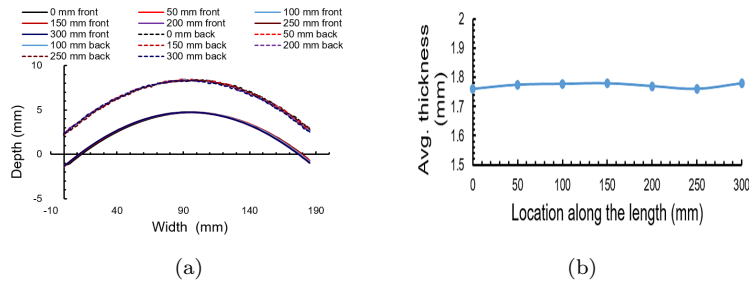
Figure 2.8: (a) Thickness variation and (b) Radius variation for UD $[0]_8$ layup
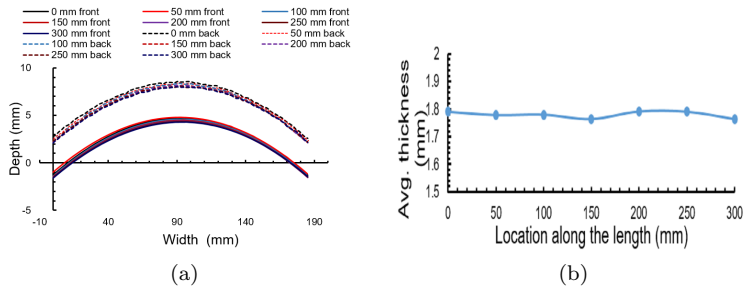
Figure 2.9: (a) Thickness variation and (b) Radius variation for cross-ply $[0/90]_4$ layup
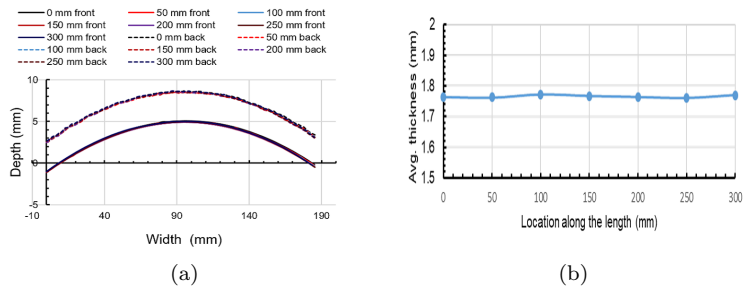
Figure 2.10: (a) Thickness variation and (b) Radius variation for Quasi-isotropic $[45/-45/90/0]_s$ layup
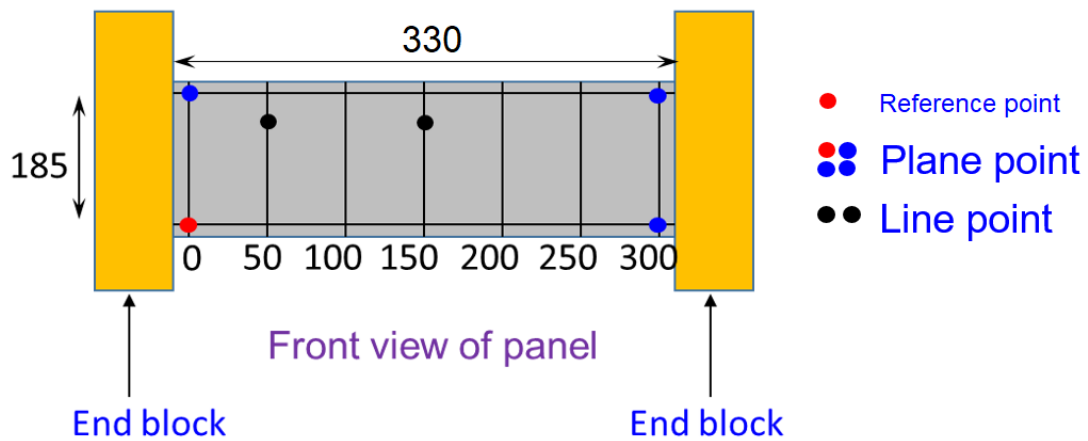
Figure 2.11: Locations of the measured points

13

2.5 Closure

This chapter mainly focused on the fabrication of the curved CFRP panel. Firstly, panels are fabricated separately by using vacuum infusion method. Further, end blocks are fabricated for applying the axial compression load. Final machining process has applied on the end block so that end blocks are parallel at their ends and also to align the geometric cross section of the curved panel cross section to coincide with loading axis of the machine after fixing in the loading fixture. Five axis CNC machine is used for parallelism of the end block.

Chapter 3

Experimental studies using DIC

3.1 Introduction

The primary aim of the present work is to investigate the pre-buckling and post-buckling behaviour of the curved CFRP panels. The secondary aim of the present study is to establish the fixtures for the simply supported boundary conditions for the curved panels. It also helped in the understanding the quality of the fabricating procedures. The experimental studies are conducted on the three curved CFRP panels with different stacking sequence (UD $[0]_8$, cross-ply $[0/90]_4$ and quasi-isotropic $[45/-45/90/0]_s$). Digital image correlation used for experiments studies to measure the whole field in-plane displacement and out-of-plane displacement of the panels subjected to axial compression loading. Experiments results are compared with the results obtained from the finite element analysis.

3.2 Curved CFRP panel testing

Comparative study of the curved CFRP panel with different stacking sequence is conducted to investigate their buckling and post-buckling behaviour under the axial compressive loading. All curved CFRP panels are made using the uni-direction carbon fibre sheet having 200 gsm. Matrix is composed of Araldite ®CY-230 Epoxy resin with Aradur HY-951 hardener in a weight ratio of $100 : 10$. The design and dimensions of the panel are shown in Figs. 1.3, 1.4 and 2.1. The different stacking sequences used for this study are listed in Table 1.1.

3.3 Experimental procedure and equipments details

Curved CFRP panel is loaded in compression using MTS Landmark ®servo-hydraulic fatigue testing machine of 100 KN capacity. The experimental setup consists of MTS load frame, digital image correlation (DIC) setup, high-speed camera, light source, image grabbing computer are shown in the Fig. 3.1. A simply supported fixture is designed and fabricated for the loading the test panels under the axial compression load. In the present study, a uni-axial compression load is applied to test panels under displacement control mode at a cross-head speed of 0.5 mm/min. Test panels are fixed into load frame and fixture such that centroid of the panel matches with the loading axis of
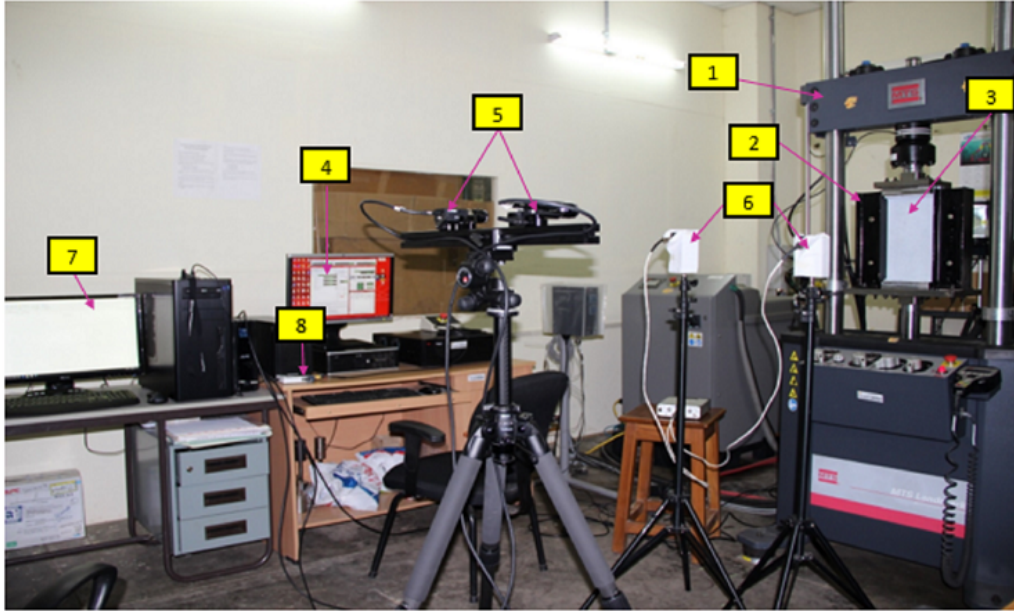
Figure 3.1: Experimental setup (1) 100 KN MTS Load frame (2) buckling fixture (3) curved CFRP test panel (4) MTS user interface (5)3D-DIC CCD cameras (6) LED light source (7) Image grabbing PC (8) NI data acquisition card

the loading machine. Top and bottom edges of the panel are clamped in the fixture whereas the straight (longitudinal) edges are supported by the simply supported condition.

The zoomed view of the specimen clamped in simple support fixture is shown in Fig. 3.2
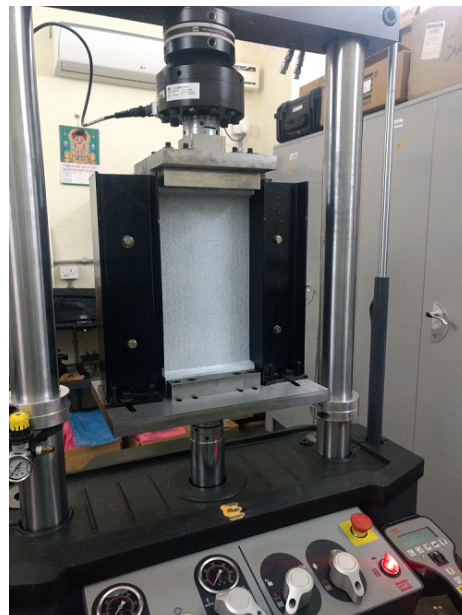
Figure 3.2: Zoomed view of clamped curved panel

3.4   3D DIC system

The DIC system consists of four Grasshopper ®CCD with a resolution of 2448 x 2048 pixels. The cameras are bounded with lenses of 17 mm focal length. Before performing the experiments, speckle pattern prepared on the curved panel surface to carry out the DIC measurement. Two sets of the LED light source were used to light up the panel surface during the testing. During testing, a camera captures five images per sec of the deformed panel and these images are then stored in the PC system. The load and displacement value corresponding to every image is taken by the MTS test system using National Instruments data acquisition system. VIC snap was software used to capture the images of the test panel during the testing. After that post-processing is done by VIC-3D software to calculate the whole-field displacement.

3.5   Post-processing

After capturing the image for each increment of load, post-processing has done by using commercially available Vic 3-D software from Correlated Solutions. The whole surface of the front side is taken as the area of interest for calculating the in-plane and out-of-plane deformation contours. Subset size is defined as 45×45 pixels, and the step size is taken 5 pixels. Filter size is used 47 which is two number higher than a subset, and it is recommended by the software provider. The tensor type used is Lagrangian. Mode shape is obtained from DIC is shown in Fig. 3.3.

(a)   (b)   (c)
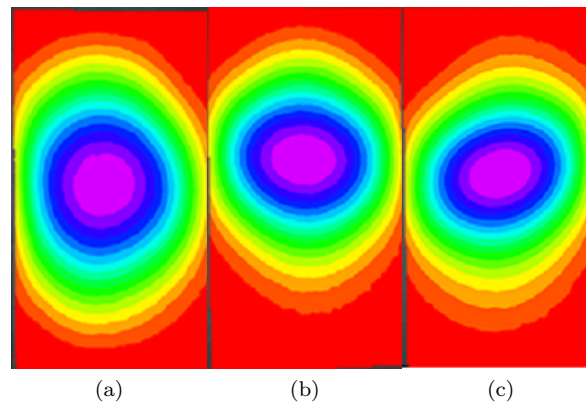
Figure 3.3: Mode shape from DIC (a) UD (b) Cross-ply (c) Quasi-isotropic

3.6   Failure in the panels

The preliminary analysis has done using FEA which shows that the quasi-isotropic $[45/-45/90/0]_s$ has the highest load carried capacity than unidirectional and cross-ply and it is well agreed with experimental observations. The stacking sequence plays the significant role in the load carrying capacity of the curved CFRP panels. For the unidirectional panel, it is observed that crack is initiated in the longitudinal direction near the simply supported edge. This crack keeps on propagating in the longitudinal direction. This formation and propagation of crack could be the result of matrix cracking. When this crack reaches to slightly above mid-plane, the fibre breakage happened along

the transverse direction indicating the failure of the panel. The failure load is 17.63 kN. This crack is highlighted in the Fig. 3.4(a).

For the cross-ply panel, it is observed that crack is propagating along the width. Then, it suddenly failed along the transverse direction slightly above the mid-plane of the panel along the loading side with a load of 12.21 kN. This crack is highlighted in the Fig. 3.4(b).

For quasi-isotropic panels, it is observed that there are two cracks developed. One of the cracks is near the curved clamped edge and propagating in the transverse direction. The other crack formed at one-fourth distance of the total length of the panel from the loading point and it is propagating in the transverse direction. These cracks are propagating due to the matrix cracking and fibre-matrix debonding. The failure load is 17.63 kN. These cracks are highlighted in the Fig. 3.4(c).

(a)

(b)

(c)
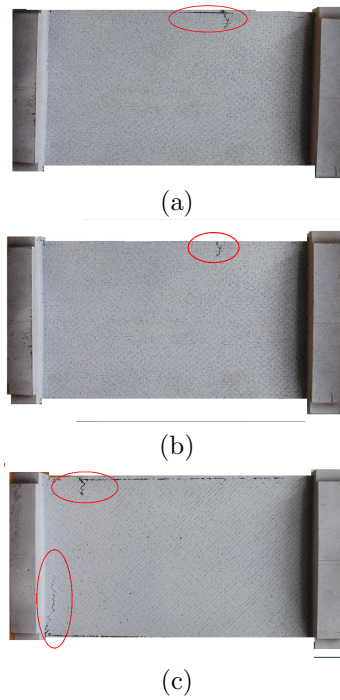
Figure 3.4: Shows the images of the collapsed panel(a)UD $[0]_8$ (b) Cross-play $[0/90]_4$ (c) Quasi-isotropic $[45/-45/90/0]_s$

3.7   Closure

Experimental studies are conducted to investigate the buckling and post-buckling behaviour of the curved CFRP panels under uni-axial compressive load with the simply supported fixture. Specimens are fabricated in-house starting with panel fabricated by the vacuum infusion method and later co-bonded with the end block for load application. Digital image correlation technique used in experimental study. Quasi-isotropic panel has higher load carrying capacity in comparison to other panels.

Chapter 4

Numerical analysis

4.1   Introduction

Numerical analysis or finite element analysis is a systematic and faster way to validate the results obtained from the experimental studies. The finite element package Abaqus-CAE 2017 used is used for this study[13]. The initial analysis is also necessary before the experimental study to predict the critical buckling and failure loads of specimen which needs to be well within the machine's maximum loading capacity. For the present study which is buckling and post-buckling of curved CFRP panel, it is required to estimate the specimen model by varying the laminate stacking sequence and geometric properties either simultaneously or separately. The finite element package Abaqus-CAE 2017 gives the flexibility to the user to analyse his model by varying different parameters of the model.

4.2   Finite element modeling of curved CFRP panel

In this section, the main focused to explain the modeling aspect of the curved CFRP panel in ABAQUS-CAE. Two different approach has been adopted for modeling the curved panel.

- Numerical analysis without initial imperfection (IMP).

- Numerical analysis with initial imperfection (IMP).

4.2.1   Numerical analysis without initial imperfection (IMP)

In this method, uniform mesh is generated using an average of the radius curvature of the panel which is obtained from the co-ordinate measuring machine (CMM). A procedure for calculating average radius of curvature is described in section 2.4.

For numerical modelling, a 3D deformable shell extrusion method is used to define the model with dimensions as shown in Fig.2.1. Three different analysis is performed based upon the stacking sequence of the panel. The stacking sequence selected for unidirectional laminate is $[0]_8$, for cross-ply laminate is $[0/90]_4$ and for the quasi-isotropic laminate is $[45/-45/-90/0]$. Each panel has 8 layers. Continuum shell element (SC8R: An 8-nodded quadrilateral in-plane general-purpose continuum shell, reduced integration with hourglass control, finite membrane strains) is selected for the analysis because it allows a high aspect ratio between in-plane dimensions and thickness changes.

Also,it is more accurate than the conventional shell element. It has 8 nodes and 3 degrees of freedom at each node, viz. three translations in the nodal x, y, and z-direction.

4.2.2 Numerical analysis with initial imperfection (IMP)

In this method, a non-uniform mesh is used which is generated by the extraction of the Digital Image Processing (DIC) data. A noble attempt is done for developing the mesh to be exact as the outer surface of the panel. So initial geometric imperfection can be captured. A procedure for extracting the data from DIC using VIC-3D software is described in the Appendix A.

For this modelling, a 3D deformable shell extrusion method is used to generate the model using DIC data and thickness as shown in Table 1.1. A conventional shell element (S4R: A 4-node doubly curved thin or thick shell, reduced integration, hourglass control, finite membrane strains.) is used for this analysis as only outer surface geometric data can be extract from the DIC. for defining the mesh control technique, quad and structure options selected to generate the mesh using to DIC data. Conventional shell element has 4 nodes and 6 degrees of freedom for each node, viz. three translational and three rotational.

4.3 CFRP laminate properties

The material properties of CFRP laminate are shown in Table 4.1. These properties are taken from M. Kashfuddoja [14].

Table 4.1: Material properties of CFRP laminate

CFRP composite laminate property		Values
In-plane properties	**Notation**	**Average of 4 specimens**
Longitudinal modulus (GPa)	E_{11}	81.9
Transverse modulus (GPa)	E_{22}	6.15
In-plane poisons ratio	ν_{12}	0.34
In-plane shear modulus (GPa)	G_{12}	2.77
In-plane Shear strength (MPa)	S_{12}	45.1
Longitudinal tensile strength (MPa)	X_T	1300
Transverse tensile strength (MPa)	Y_T	22.97
Longitudinal compressive strength (MPa)	X_C	640
Transverse compressive strength (MPa)	Y_C	93.2
Out-of-plane properties		**Value**
Out-of-plane poisons ratio	ν_{23}	0.50
Out-of-plane shear modulus (GPa)	G_{23}	2.05

4.4   Loading condition

The end block attached to the curved edge of the panel with resin. To these attached end block the load is applied during experimentation. To reproduce the same boundary condition in numerical model, all nodes those are representing the fixed edge in the experiment are given as clamped boundary conditions, thereby restricting the all degrees of freedom, in numerical model. All nodes at the loading edge are tied with a reference point in the axial direction and compressive load is applied to the reference point. And only out-of-plane deformation is restricted to the straight egde of the panel. All these applied boundary conditions for the panel are described in Fig. 4.1(a).
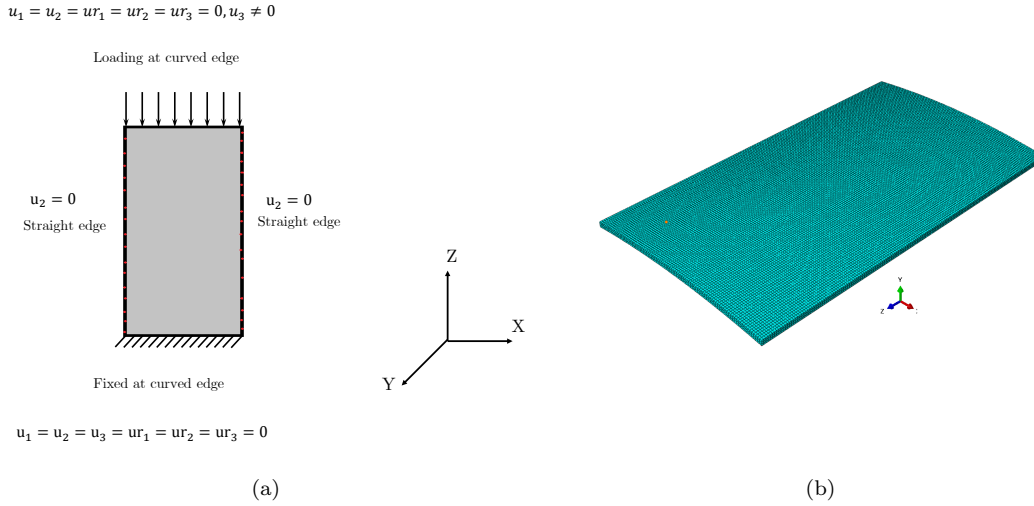

Figure 4.1: (a)Boundary conditions of curved CFRP panels (b) mesh of curved model

4.5   Mesh convergence study

Mesh convergence study is performed based upon the first eigenvalues of linear buckling analysis. The best mesh size obtained for the mesh is 2 mm× 2 mm and sweep technique used to assign mesh control to the curved object. Finite element meshed model is shown in Fig. 4.1(b). The mesh convergence study plot is shown in the Fig.4.2.

4.6   Eigen buckling analysis

The initial stage of buckling is linear or eigen buckling analysis in finite element analysis(FEA). To forecasting the theoretical buckling strength of an elastic structure in FEA, linear buckling analysis is done. The critical buckling load of the composite panels is estimated using the eigenvalue buckling analysis. The applied load is multiply with the critical load factor to obtained the critical buckling load.

$$\text{Buckling load} = \text{Eigen value} \times \text{applied load.} \tag{4.1}$$

In this analysis,non-linearities and and particular initial geometric imperfections do not consider.
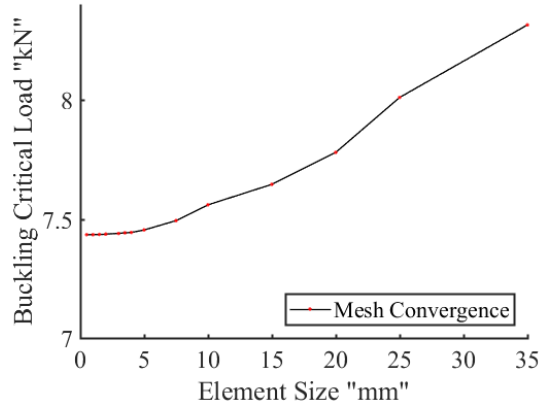
Figure 4.2: Mesh convergence study

But for performing the riks analysis or post-buckling analysis, a binary file is known as .fil file required which is generated by using the following syntax in the software during the linear buckling analysis.

```
* NODE FILE, GLOBAL = YES, LAST MODE = 10
U
```

4.6.1 Buckling loads

For the buckling analysis, an external load of 1 KN is applied and linear buckling analysis is performed. Afterwords critical load factor estimated using subspace eigensolver. For calculating the first ten buckling loads, vectors used per iteration are 18. The first ten buckling loads obtained are listed in Table 4.2.

Table 4.2: Buckling load at different mode shape

| Sr.no | Mode-1 | Critical buckling load (kN) | | | | | |
| | | Unidirectional $[0]_8$ | | Cross-ply $[0/90]_4$ | | Quasi-isotropic $[45/-45/90/0]_s$ | |
		with Initial IMP	without Initial IMP	with Initial IMP	without Initial IMP	with Initial IMP	without Initial IMP
1	Mode-1	6.5162	7.6027	7.2482	8.6491	11.991	14.034
2	Mode-2	8.5390	9.4783	7.6332	8.7602	12.566	14.285
3	Mode-3	9.4170	10.035	11.114	11.785	13.525	14.513
4	Mode-4	9.9081	10.507	13.028	12.962	14.203	15.096
5	Mode-5	13.267	14.296	13.479	13.443	16.284	16.642
6	Mode-6	15.251	15.985	13.643	13.747	17.373	17.384
7	Mode-7	16.744	17.239	17.946	17.466	19.491	20.029
8	Mode-8	16.851	17.574	18.229	17.525	19.642	20.070
9	Mode-9	17.977	19.185	18.373	17.751	20.379	20.193
10	Mode-10	18.811	19.833	22.217	21.407	21.785	21.362

4.6.2 Buckling mode shapes

Mode shapes obtained from the linear buckling analysis are arranged for the first four buckling loads in figure for all three case. It is observed that maximum out-of-plane deformation occur at the centre of the each panel due the simply support condition and it increases along the longitudinal axis of

22

the panel from one to four location for UD $[0]_8$ as shown in Fig. 4.3 and it is moved to two, three for the second and third mode shape respectively but it is suddenly jumped to six for the fourth mode shape for cross-ply $[0/90]_4$as shown in Fig. 4.4. For quasi-isotropic $[45/-45/90/0]_s$, out of plane deformation remain near the centre of the panel for second and third mode shape but it occurs one-fourth and third-fourth location along the length for mode shape as shown in Fig. 4.5.
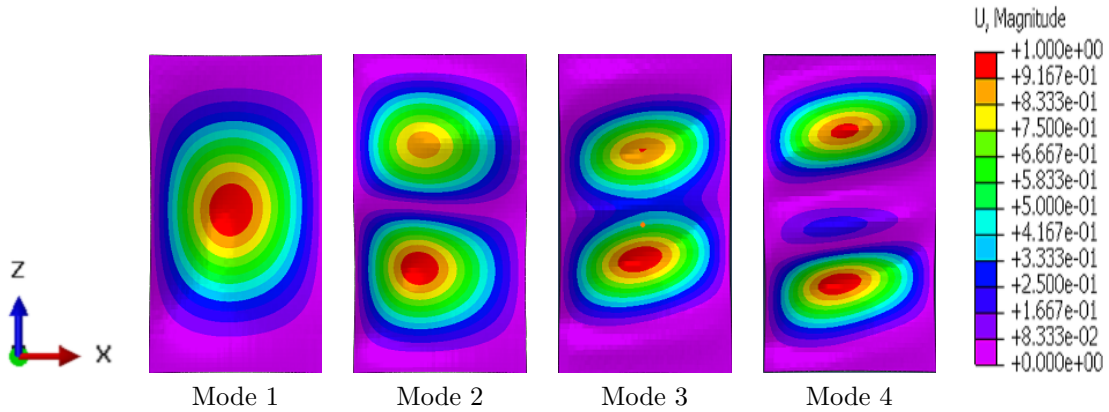

Figure 4.3: Unidirectional laminate $[0]_8$ mode shape obtained from eigen value analysis without initial imperfection.
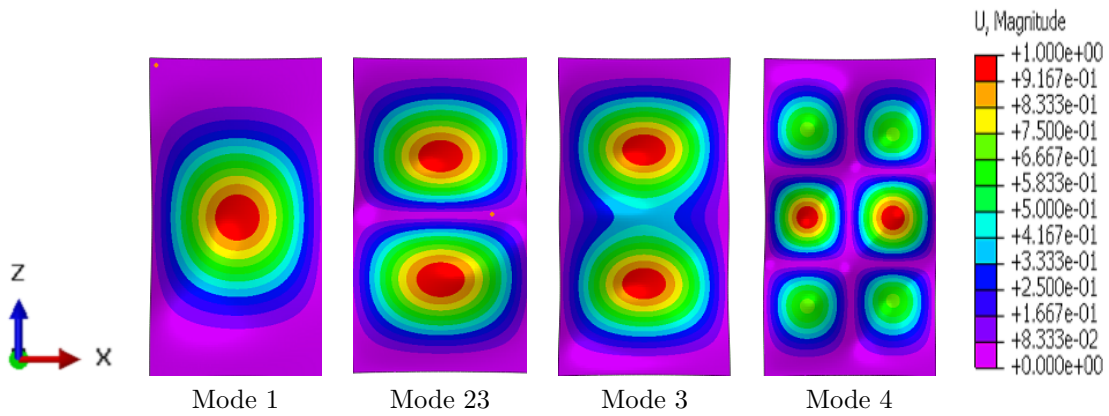

Figure 4.4: Cross-ply laminate $[0/90]_4$ mode shape obtained from eigen value analysis without initial imperfection.
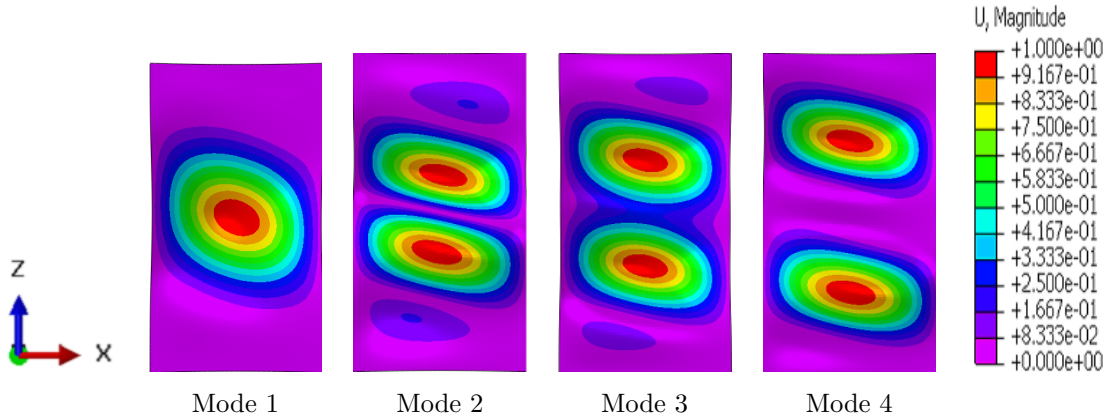
Figure 4.5: Quasi-isotropic laminate $[45/-45/90/0]_s$ mode shape obtained from eigen value analysis without initial imperfection.

4.7   Post-buckling analysis

The critical buckling load obtained from the linear buckling analysis generally higher than the actual buckling load for the structure. It is due to imperfection sensitivity and it is very critical for the thin walled shell structures. Linear buckling analysis predicts only the critical buckling loads. The post-buckling behaviour of the structure cannot determine by the eigen value analysis. So non-linear post-buckling analysis is performed to obtained the buckling response after that critical load. Axial load versus end shortening behaviour of the structure can be obtained by the post-buckling. It is also give the out-of plane deformation response, in-plane deformation response and stress distribution of the whole region of the panel at the each incremental of the load. In reality, structures are not perfect, they have some initial imperfection such as thickness and radius variation, load eccentricity etc. An initial imperfection is required for performing the post-buckling analysis which is given by the binary file generated during the linear buckling analysis. Riks method is used for post-buckling analysis [15]. In this analysis, initial geometric imperfection and non-linearities are considered. The imperfection file is generated by eigen value analysis. This file is used for post-buckling analysis by giving the following syntax in the Abaqus input file:

```
* IMPERFECTION, FILE= <IMPERFECTIONFILENAME>, STEP=1
* 1, numerical value of 5 % of thickness
```

4.8   Closure

The curved CFRP panel with three different stacking sequence has been modelled and analyzed by the finite element commercial software Abaqus-CAE 2017 by two different approach. The buckling mode shape obtained from the linear buckling analysis and mode shape have presented for each case. The post-buckling analysis has performed by the static, Rik's method to obtain the non-linear behavior of the panel. Imperfection corresponds to the 5 % of the thickness.

Chapter 5

Results and discussions

5.1 Introduction

This chapter deals with observations from the conducted experimental study to investigate the stability behavior of the curved CFRP panels under axial compression load. For the processing of the experimental results VIC 3D software used.

5.2 Numerical results

5.2.1 Eigen buckling analysis results

Eigen buckling mode shapes are obtained from the finite element analysis as shown in Figs. 4.3, 4.4, and 4.5. These analysis are carried out using the finite element software Abaqus-CAE 2017. Buckling load is obtained from the eigen values using Eq. 4.1.

In the linear buckling analysis, first eigen value gives the critical buckling load. The critical buckling load obtained from the numerical analysis with and without initial imperfections, for a unidirectional curved panel is 6.512 kN and 7.60 kN, for a cross-ply panel is 7.24 kN and 8.64 kN and for quasi-isotropic laminate is 11.99 kN and 14.034 kN. The buckling load for different mode shapes is listed in the Table 4.2.

5.2.2 Post-buckling results

The non-linear response of the UD $[0]_8$, cross-ply $[0/90]_4$ and quasi-isotropic $[45/-45/-90/0]_s$ laminates with simply supported boundary condition is shown in Fig. 5.1. The horizontal axis represents the axial displacement and vertical axis represents the axial compression load. Axial load versus end shortening curve is linear in the pre-buckling region. The UD panel buckled at 10.64 kN load and after the drastic reduction of 4.9 kN of load, post-buckling is started. The slope of load versus end shortening curve is higher for the pre-buckling region in comparison to the post-buckling region because after the buckling, specimen losses its stiffness.
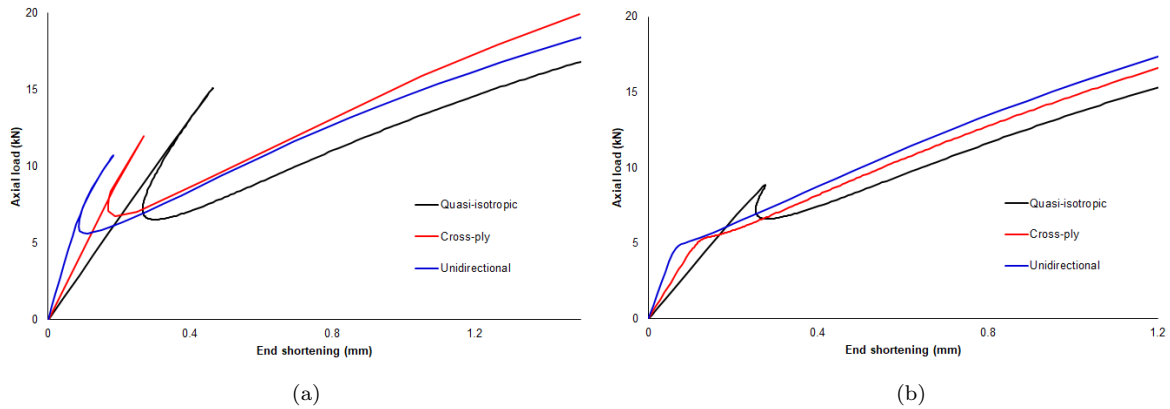
Figure 5.1: Load vs. displacement response of curved composite panel obtained from finite element analysis (a) without initial imperfection (b) with initial imperfection

5.2.3 Out-of-plane deformation results

Out-of-plane deformations obtained from the numeral analysis without initial imperfection are shown in Figs. 5.3(b), 5.4(b) and 5.5(b) for UD $[0]_8$, 5.6(b), 5.7(b) for cross-ply $[0/90]_4$ and 5.8(b), 5.9(b) and 5.10(b) for quasi-isotropic $[45/-45/-90/0]_s$ respectively. The out-of-plane deformations obtained from the numeral analysis with initial imperfection are shown in Figs. 5.3(c), 5.4(c) and 5.5(c) for UD $[0]_8$, 5.6(c),5.7(c) for cross-ply $[0/90]_4$ and 5.8(c) ,5.9(c) and 5.10(c) for quasi-isotropic $[45/-45/-90/0]_s$ respectively. The maximum out-of-plane deformation observed at the centre of each panel due to simply supported boundary condition. In the figures, the contours are displayed at the different increasing load. It is observed that the contours obtained form the numerical results are symmetric along the both axis, i.e. longitudinal and transverse.

5.2.4 In-plane deformation results

In-plane deformations obtained from the numeral analysis without initial imperfection are shown in Figs. 5.11(b), 5.12(b) and 5.13(b) for UD $[0]_8$, 5.14(b), 5.15(b) for cross-ply $[0/90]_4$ and 5.16(b), 5.17(b) and 5.18(b) for quasi-isotropic $[45/-45/-90/0]_s$ respectively. The in-plane deformation obtained from the numeral analysis with initial imperfection is shown in figure 5.11 (c),5.12 (c)and 5.13 (c) for UD $[0]_8$, 5.14 (c),5.15 (c) for cross-ply $[0/90]_4$ and 5.16(c) ,5.17 (c) and 5.18 (c) for quasi-isotropic $[45/-45/-90/0]_s$ respectively.it is observed that contours obtained form the numerical results are perfectly symmetric along the only longitudinal axis.

5.3 Experimental results

5.3.1 Out-of-plane deformation result

Out-of-plane deformations obtained from the DIC experiments are shown in Figs. 5.3(a), 5.4(a) and 5.5(a) for UD $[0]_8$, 5.6(a), 5.7(a) for cross-ply $[0/90]_4$ and 5.8(a), 5.9(a) and 5.10 (a) for quasi-isotropic $[45/-45/-90/0]_s$ respectively. It is observed that out-of-plane contours propagate as the half sine wave along the longitudinal direction. Out-of-plane displacement at the centre of the

panels more significant with the increase of load and the mode shape remains like until the failure of panels. These contours are symmetric about the axes.

5.3.2   In-plane deformation results

In-plane deformations obtained from the experiment (DIC) are shown in Figs. 5.11(a), 5.12(a) and 5.13(a) for UD $[0]_8$, 5.14(a), 5.15(a) for cross-ply $[0/90]_4$ and 5.16(a), 5.17(a) and 5.18(a) for quasi-isotropic $[45/-45/-90/0]_s$ respectively. It is observed that contours obtained form the DIC results are symmetric along the only longitudinal axis but as load is increasing, contours are obtaining the symmetric along the both axis.

5.3.3   Load versus end shortening

The load versus displacement behaviour plot obtained from the experimental data is shown in Fig. 5.2. The pre-buckling stiffness for UD $[0]_8$, cross-ply $[0/90]_4$, quasi-isotropic $[45/-45/-90/0]_s$ is 50.12 kN/mm, 41.58 kN/mm and 31.48kN/mm respectively. Stiffness values obtained from the numerical analysis with and without initial imperfection and experiments are listed in the Table 5.1.The axial stiffness of the unidirectional laminate is the highest because the orientation of the fiber is along the loading direction.
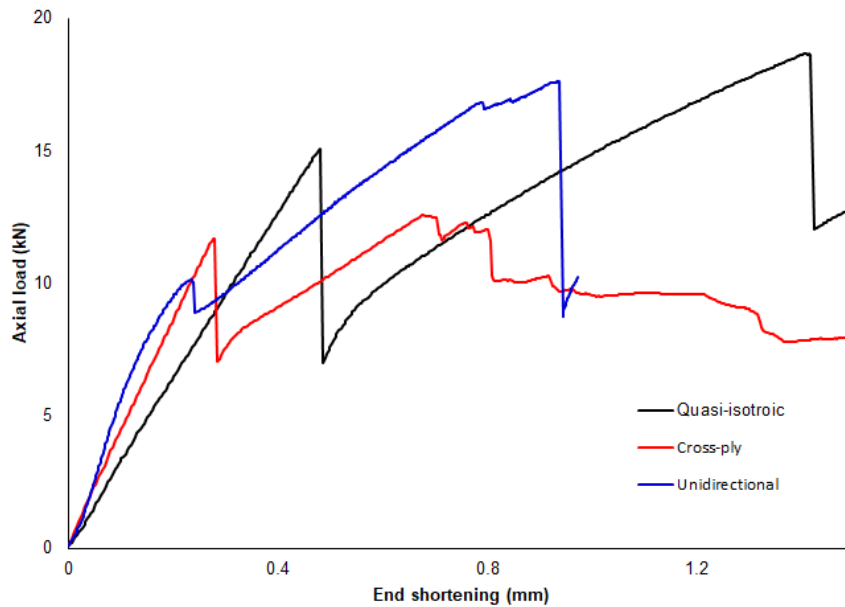

Figure 5.2: Load vs. displacement response of curved CFRP panels under axial compression load obtained from experiment

Table 5.1: Axial stiffness of the curved specimen

laminate	Pre-buckling stiffness (kN/mm)			Post-buckling stiffness (kN/mm)		
	Exp.	Numerical with Intial Imperfection	Numerical without Intial Imperfection	Exp.	Numerical with Intial Imperfection	Numerical without Intial Imperfection
Quasi-isotropic $[45/-45/90/0]_s$	31.48	32.58	32.88	11.64	10.16	9.80
Cross-ply $[0/90]_4$	41.58	44.57	43.21	12.62	10.77	11.77
UD $[0]_8$	50.12	56.63	60.12	13.29	11.03	11.69

5.4 Comparison of experimental and numerical results

The comparison between numerical analysis and experimental analysis is shown in figure (5.3-5.18). Load versus end shortening displacement comparison between UD and quasi-isotropic laminate is shown in figure 5.19.Experimental results are very close to the numerical results in the pre-buckling and post-buckling region. For the buckling region,there is only 3.3 % for quasi-isotropic, 6.7% for cross ply and 11.49 % unidirectional laminate stiffness difference between numerical and experimental results.Load decrease to 11.13 % ,37.25 % and 50.02 % for the UD,cross-ply and quasi-isotropic laminate respectively during the sudden mode transition.

Out-of-plane displacement and in-plabe displacement comparison is shown in figure (5.3,5.4,5.5), (5.6,5.7) and (5.8,5.9,5.10)for UD and cross-ply quasi-isotropic laminate. These comparison made at the different the buckling load. The maximum out-of plane displacement has 0.12 % , 3.02 % and 21 % difference for UD at 15.21 kN load , for cross-ply at 10kN load and for quasi-isotropic laminate at 14.67 kN load respectively.

The maximum in-plane displacement has 1.4 % , 2.02 % and 1.6 % difference for UD at 15.21 kN load , for cross-ply at 10kN load and for quasi-isotropic laminate at 14.67 kN load respectively.

Table 5.2: Summary of buckling and post-buckling results of curved CFRP panels obtained from experimental result

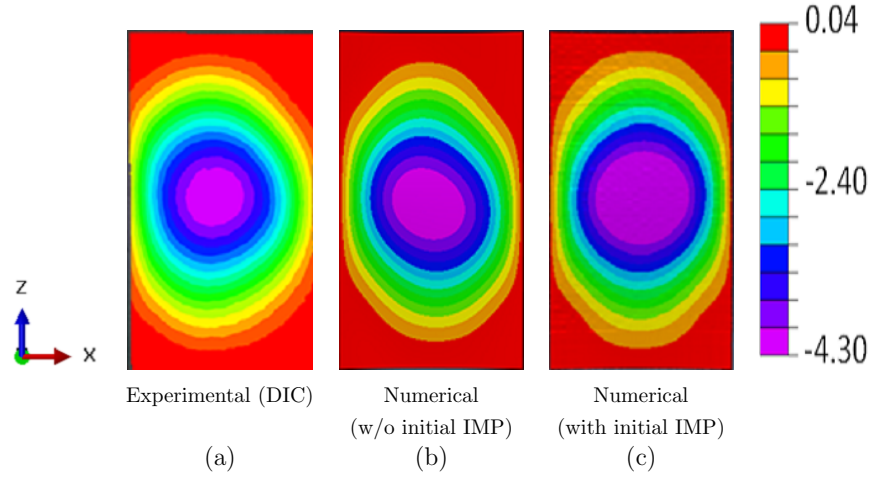| Specimen / quantity	Unidirectional $[0]_8$	Cross ply $[0/90]4$	Quasi-isotropic $[45/-45/90/0]_s$
Buckling load (kN)	10.09	11.65	15.068
Failure load (kN)	17.63	12.21	18.631
Max end shortening displacement (mm)	0.971	1.6	1.497

Figure 5.3: Out of deformation contours at 10 kN for Unidirectional laminate $[0]_8$
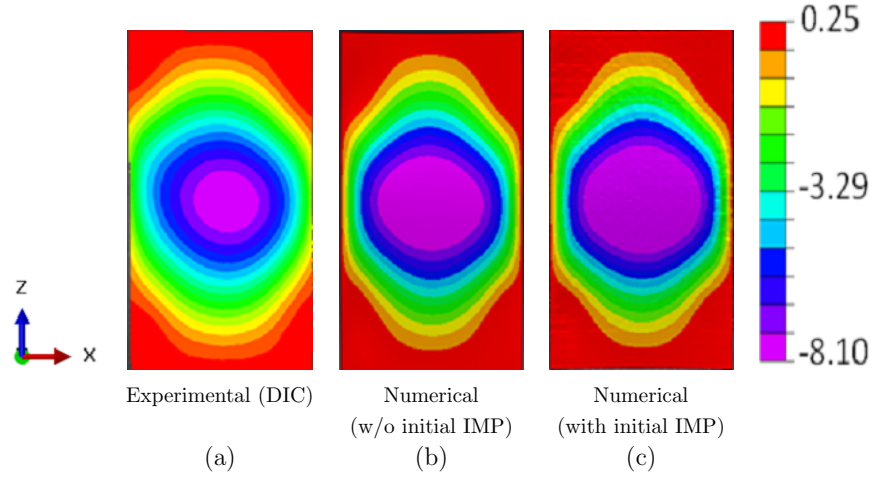

Figure 5.4: Out of deformation contours at 14.5 kN for Unidirectional laminate $[0]_8$
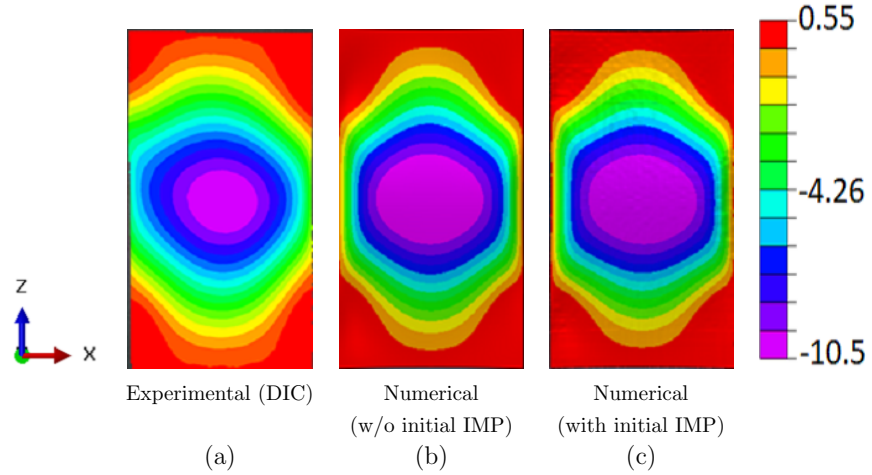

Figure 5.5: Out of deformation contours at 18.3 kN for Unidirectional laminate $[0]_8$
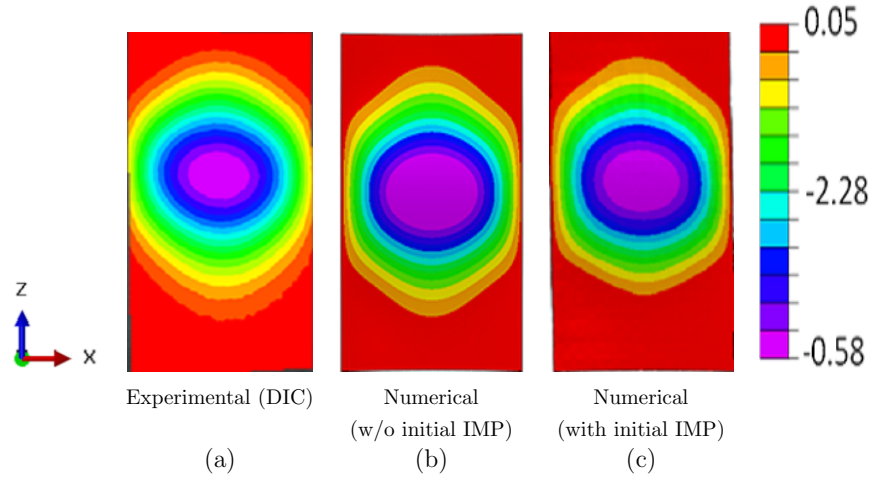
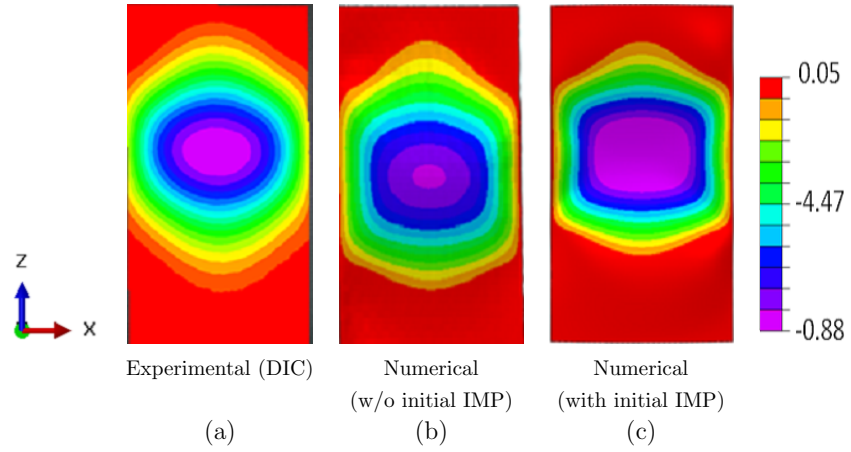Figure 5.6: Out of plane deformation contours at 10 kN for cross-ply $[0/90_4]$

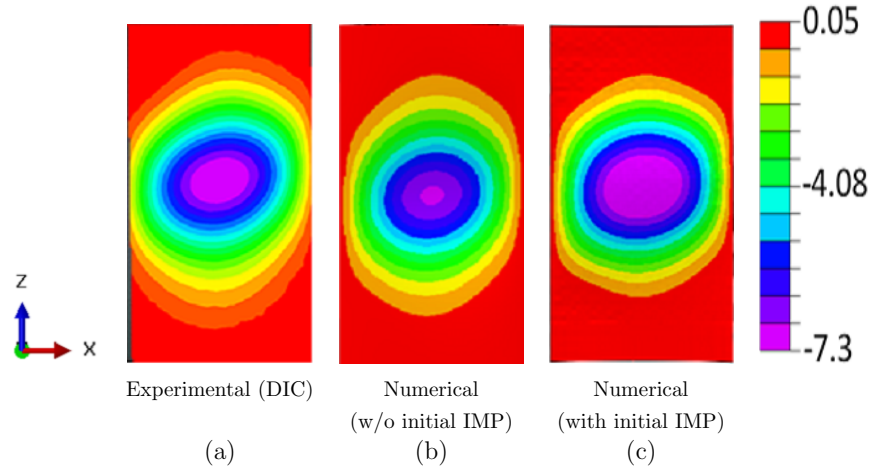Figure 5.7: Out of plane deformation contours at 14.5 kN for cross-ply $[0/90_4]]$

Figure 5.8: Out of plane deformation contours at 10 kN for Quasi-isotropic $[45/-45/90/0]_s$

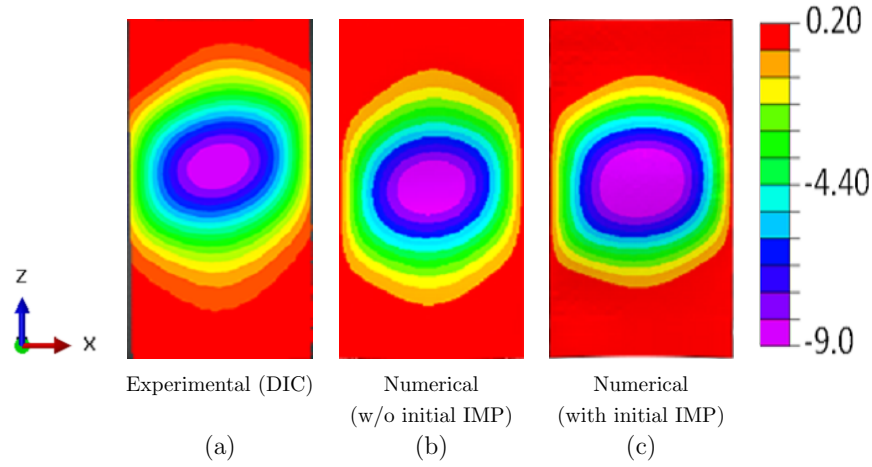

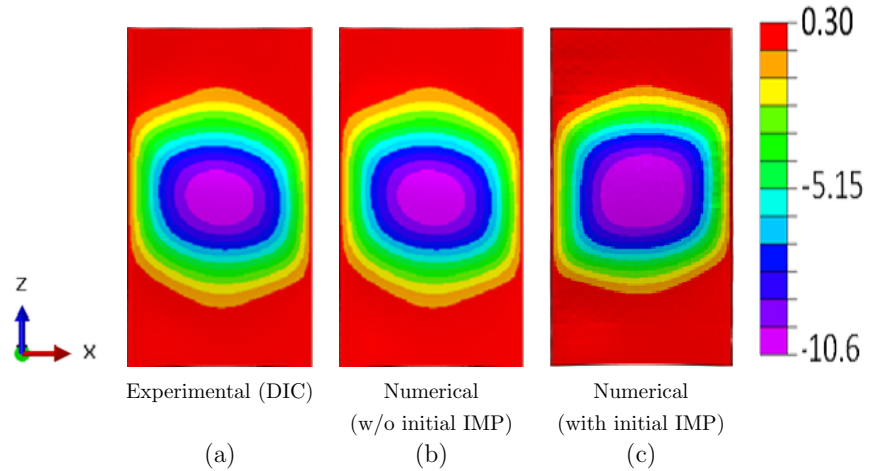Figure 5.9: Out of plane deformation contours at 14.5 kN for Quasi-isotropic $[45/-45/90/0]_s$

Figure 5.10: Out of plane deformation contours at 18.3 kN for Quasi-isotropic $[45/-45/90/0]_s$
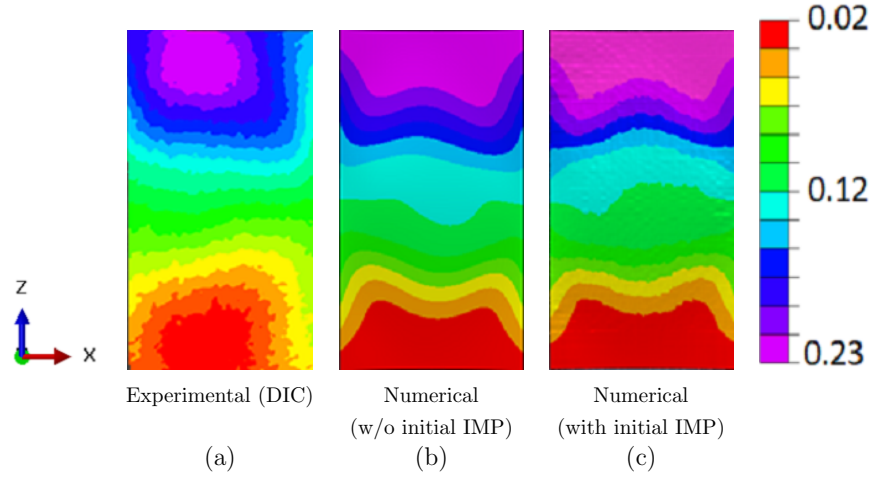
Figure 5.11: In-plane deformation contours at 10 kN for Unidirectional laminate $[0]_8$
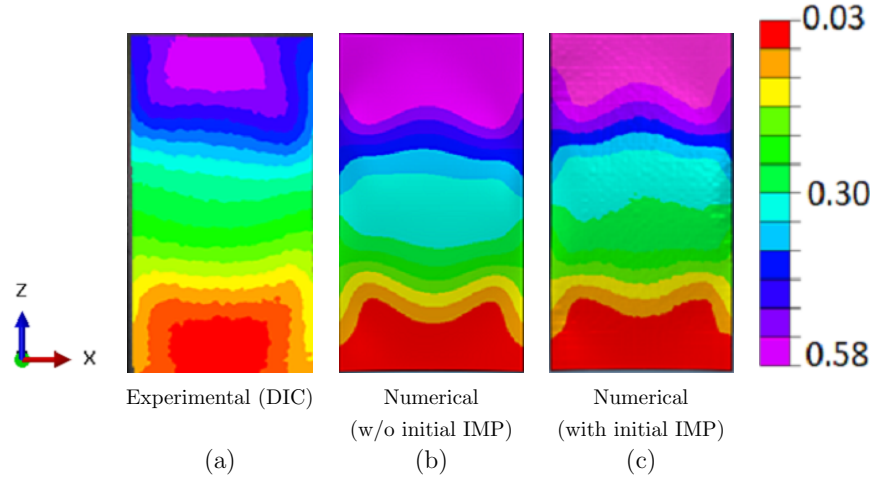

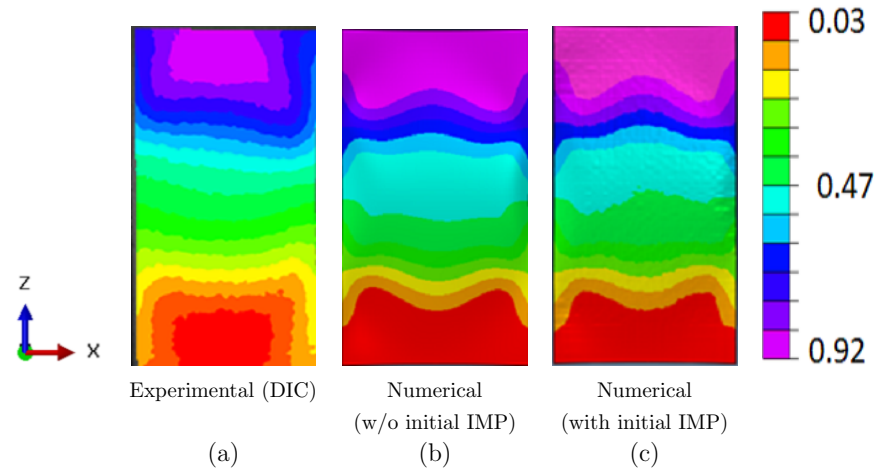Figure 5.12: In-plane deformation contours at 14.5 kN for Unidirectional laminate $[0]_8$

Figure 5.13: In-plane deformation contours at 18.3 kN for Unidirectional laminate $[0]_8$

Figure 5.14: In-plane deformation contours at 10 kN for Cross-ply $[0/90]_4$
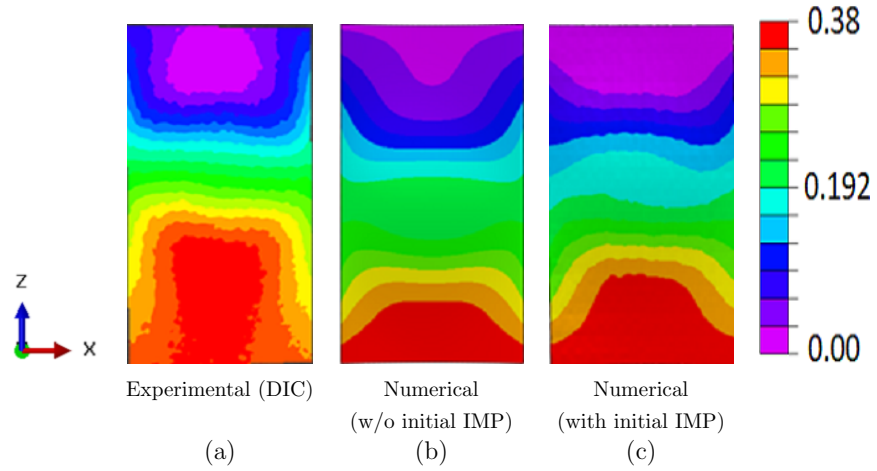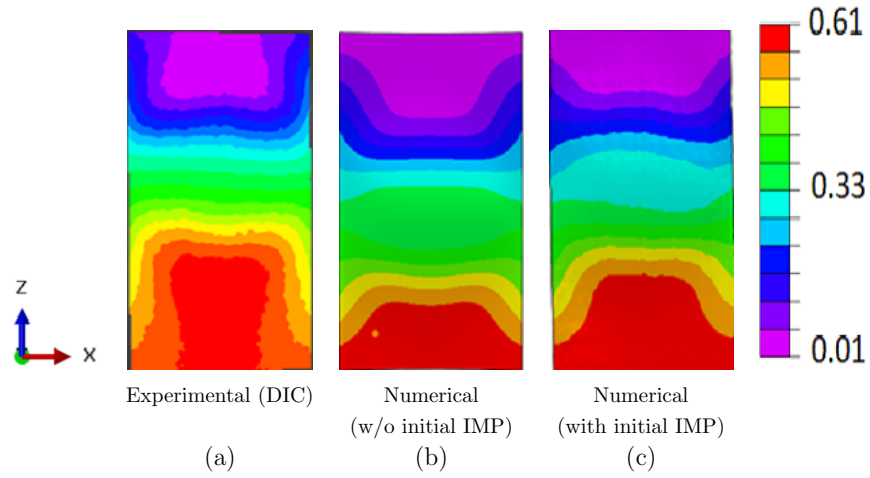

Figure 5.15: In-plane deformation contours at 14.5 kN for Cross-ply $[0/90]_4$
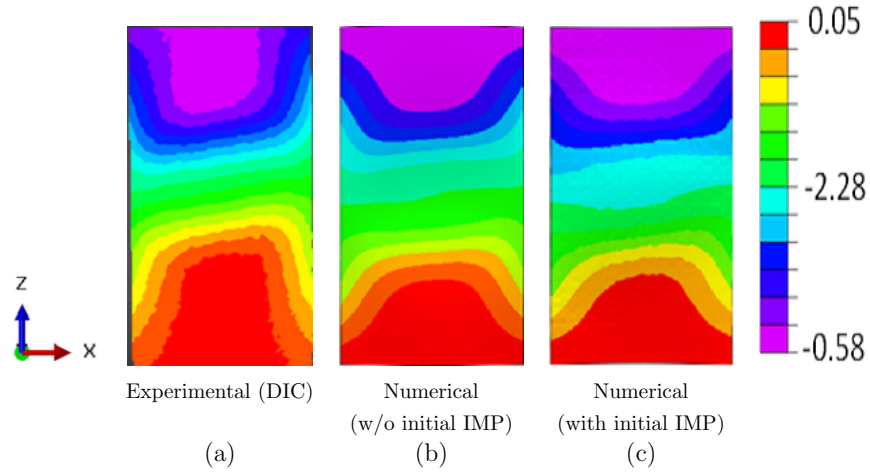
Figure 5.16: In-plane deformation contours at 10 kN for Quasi-isotropic $[45/-45/90/0]_s$
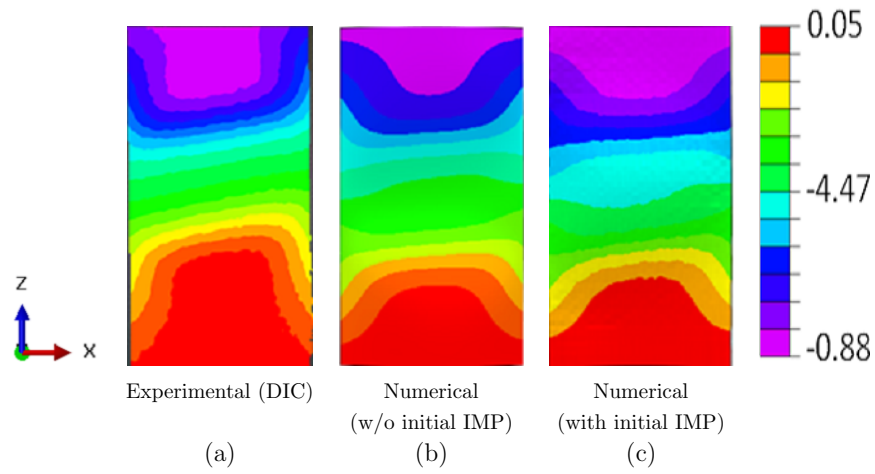

Figure 5.17: In-plane deformation contours at 14.5 kN for Quasi-isotropic $[45/-45/90/0]_s$
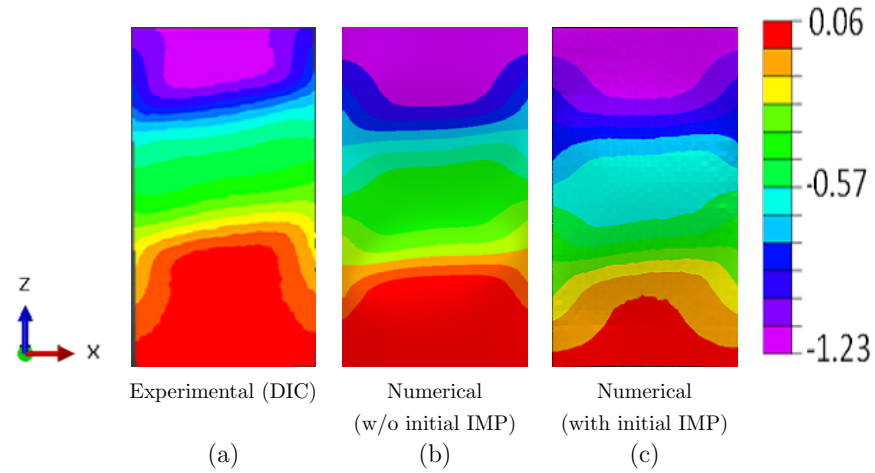

Figure 5.18: In-plane deformation contours at 18.3 kN for Quasi-isotropic $[45/-45/90/0]_s$
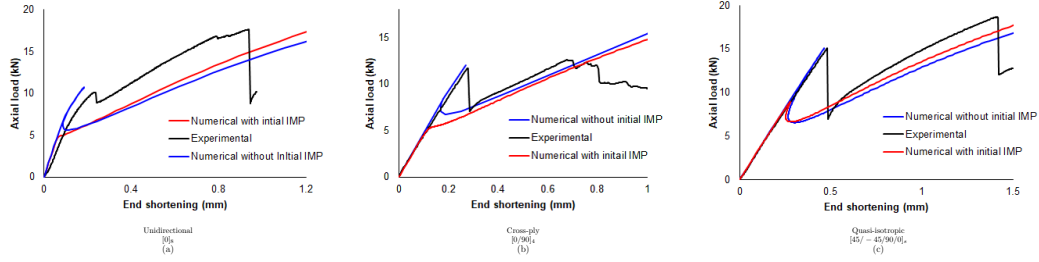
Figure 5.19: Load vs. displacement behaviour comparision between experimetal and numerical result

5.5 Closure

Experimental results validate with numerical results which are close to each other. Axial stiffness of quasi-isotropic laminate obtained from numerical is very close to the experimental with error 3.3 % in the pre-buckling region and 12.71 % in the post-buckling region. Axial stiffness of cross-ply laminate obtained from numerical is close to the experimental with error 6.7 % in the pre-buckling region and 14.65 % in the post-buckling region. Axial stiffness of unidirectional laminate obtained from numerical is close to the experimental with error 11.49 % in the pre-buckling region and 17 % in the post-buckling region. The error is maximum in the unidirectional laminate which due to the fabrication. Out-of-plane deformations contours obtained from experimental results are similar to that of numerical results. The maximum out-of-plane is found at the centre of each panel. In-plane deformations contours obtained from experimental results are following the same trend that of numerical results. The buckling load of the unidirectional laminate is the lowest because there is no coupling between the extensional and bending stiffness matrix because the value of all elements for UD laminate bending matrix are zeros. It is observed that buckling load depends upon the stacking sequence of the laminate. There is no much significant influence of the numerical analysis with initial imperfection on the axial stiffness of the panel. So it means that the axial stiffness of the panel does not depend upon the imperfection factor. On the other hand, first buckling load of each stacking sequence came near about half of the first buckling load without initial imperfection. Buckling load highly depends upon the imperfection of the panel.

Chapter 6

Conclusion and future work

6.1 Conclusion

In the present study, three different curved CFRP panels are fabricated in-house and tested under the axial compression load. The initial imperfection of the panels is measured by using CMM machine, and the average values of thickness and radius of curvature obtained from the CMM measurements are used in the finite element analysis. To obtain the initial geometry, DIC data collected from actual panels used for testings, are imported into Abaqus for modelling the curved panel. MATLAB is used for importing the data from DIC to FEA. Two different types of FEA are carried out.

- Finite Element Analysis (FEA) with initial imperfection.

- Finite Element Analysis (FEA) without initial imperfection.

The critical load, buckling mode shapes, buckling and post-buckling response was captured using finite element analysis software Abaqus-CAE 2017 and validated with the experimental results. The experimental study was carried out by the DIC method.
It is observed that there is a sudden mode transition with a load reduction during the buckling of the panels. The panels are failed along the width of the panels slightly above the half height from the bottom edge. The crack is initiated because of matrix cracking and followed by the fibre breakage indicates the failure of the panel. It is observed that the load carrying capacity is the highest for the quasi-isotropic laminate and the lowest for unidirectional laminate.
The stiffness of the panel calculated from FEA with and without initial imperfection is close to that of experimental for the pre-buckling and post-buckling region. This indicates that stiffness depends upon the material properties, but it does not depend upon the mesh. The Critical buckling load calculated for the FEA without initial imperfection is close to that of the experimental value. But critical buckling load obtained from the FEA with initial imperfection is half of the experimental value. This indicates that the critical buckling load is highly depends upon the mesh during the FEA. A uniform mesh generated for FEA without initial imperfection and non-uniform mesh generated for FEA with initial imperfection, it is because the outer surface of the panel is not uniform. There is a good agreement in DIC and FEA, for out-of-plane contours but significant difference in in-plane displacement contours. It is the basic study on the curved panel and results are matched in buckling

and post-buckling region. Hence it can be concluded that fixture setup, application of load and fabrication method are good.

6.2   Future work

After the successful study of the buckling and post-buckling of curved composite panel. some recommendations are following based upon the current work.

- In this thesis, damage analysis is not considered in the numerical simulation. Further research with failure criterion input is required for doing the damage analysis and in order to have a more meaningful validation results with experiments.

- In the present work, boundary conditions of the curved composite plate were considered as simply supported along the straight edge of specimen and fixed along the curved edge for simplification. For further assessments, one can play with different-different boundaries condition which may be realistic in the nature.

- In the present work, only uni-axial load is taken in account. For further work, bi-axial compressive loading, shear loading and thermal loading can be considered and effect of buckling and post-buckling may be studied.

- The effect of the cut-outs in the curved composite plate can be study.

Appendix A

Mesh generation with DIC points

A.1 Introduction

The final objective of the present work is modelling of the curved panels with the DIC(Digital Image Processing) so initial geometric imperfection can be obtained during the simulation. For each tested panels, DIC data used to generate the finite element (Abaqus) meshes representative of its initial geometry.

A.2 Procedure

The procedure of the modelling of the curved panels by using of the DIC data is following [16].

- Open the project (.Z3D) file in Vic-3D.

- Display the co-relation data at 0 kN load (first speckle image).

- Show the 2D plot and set the contours variable as Y[mm].

- Now, go to the inspector tools and select the inspect line as shown in the figure A.1 (a) and draw the line in area of interest (AOI) at every 5 mm as shown in figure A.1 (b) and the drawing direction of line should be same as the first line and we can track the location of the cursor at the right down corner of the display window which helps for drawing the line at particular location.

- Now, click on the extract button to extract data as shown in figure A.2.

- Click on the save data and tick only X, Y and Z in variables column and first file in data files column and then press ok and save the file as (filename.csv) as shown in figure A.3.

- Store the X, Y and Z data in Matlab.

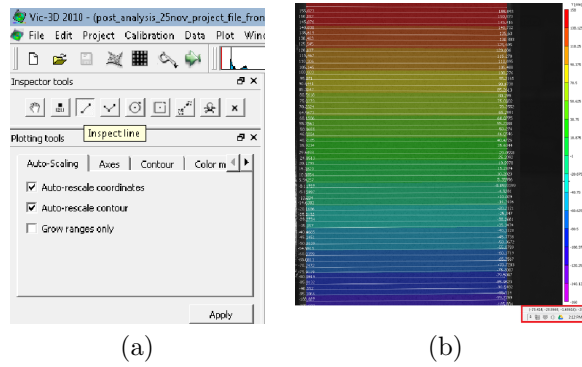- follow the flow chart as shown in figure A.4.

Figure A.1: (a) Position of inspect line in the Vic-3D (b) Data line at every 5 mm
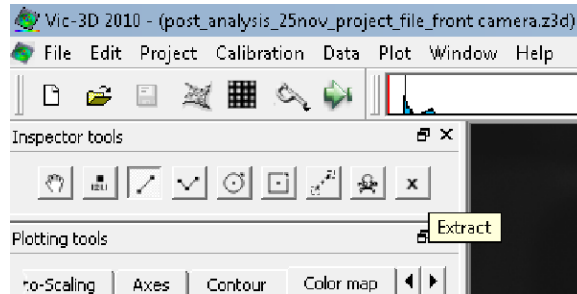

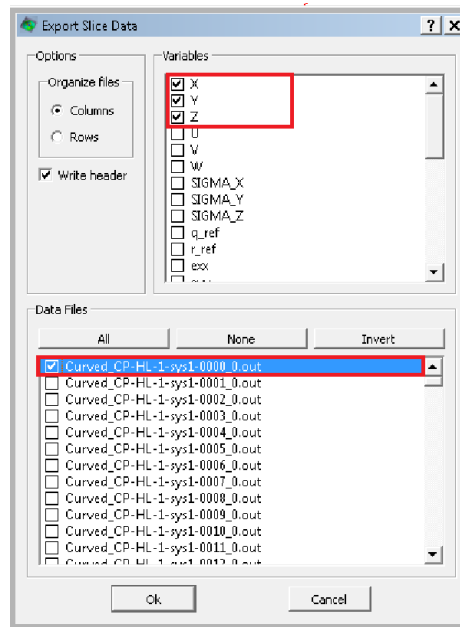Figure A.2: Location of the extract button in Vic-3D software

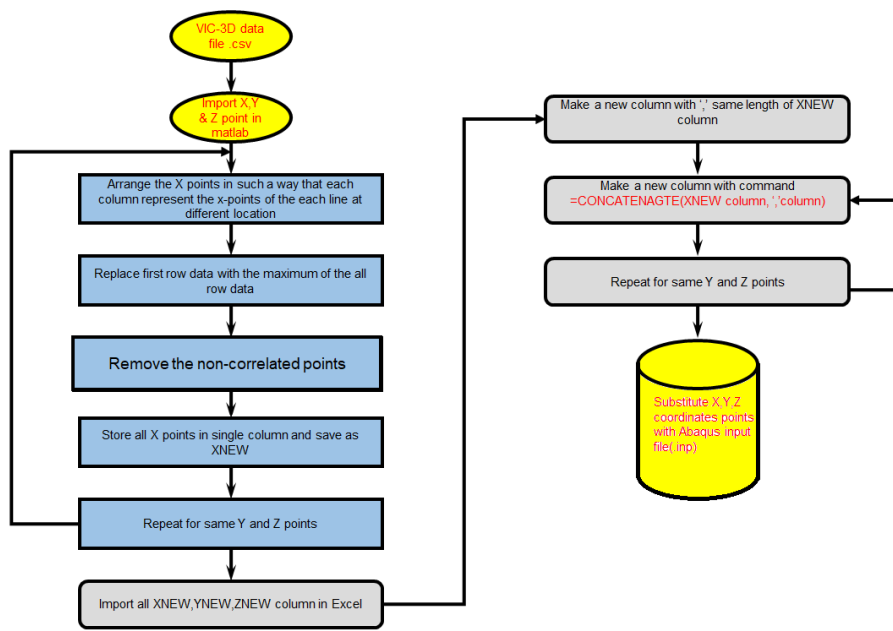Figure A.3: Pop up window for the extract the point from the Vic-3D.

Figure A.4: Meshing alogorithm

References

[1] R. P. Thornburgh. Imperfection and Thickness Measurement of Panels Using a Coordinate Measurement Machine .

[2] N. Panzeri and C. Poggi. Influence of geometric imperfections and lamination defects on the buckling behaviour of composite cylinders. In Proceedings of Second International Conference on Thin-Walled structures, NE Shanmugan et al. eds., Elsevier. 1998 279–287.

[3] N. R. Bauld and N. S. Khot. A numerical and experimental investigation of the buckling behavior of composite panels. *Computers & Structures* 15, (1982) 393–403.

[4] N. Breivik and M. Hyer. Buckling and postbuckling behavior of curved composite panels due to thermal and mechanical loading. *Journal of reinforced plastics and composites* 17, (1998) 1292–1306.

[5] J. Starnes, N. Knight, and M. Rouse. Postbuckling behavior of selected flat stiffened graphite-epoxy panels loaded in compression. *AIAA journal* 23, (1985) 1236–1246.

[6] N. Khot. Buckling and postbuckling behavior of composite cylindrical shells under axial compression. *AIAA journal* 8, (1970) 229–235.

[7] K. Kim. Buckling behaviour of composite panels using the finite element method. *Composite structures* 36, (1996) 33–43.

[8] M. L. Aparna, G. Chaitanya, K. Srinivas, and J. A. Rao. Fabrication of Continuous GFRP Composites using Vacuum Bag Moulding Process. *International Journal of Advanced Science and Technology* 87, (2016) 37–46.

[9] C. Featherston. Geometric Imperfection Sensitivity of Curved Panels Under Combined Compression and In-Plane Bending–A Study Using Adaptive Meshing and DIC. *Strain* 48, (2012) 286–295.

[10] C. A. Featherston, M. J. Eaton, and K. M. Holford. Modelling the Effects of Geometric Imperfections on the Buckling and Initial Post-buckling Behaviour of Flat Plates Under Compression Using Measured Data. *Strain* 48, (2012) 208–215.

[11] R. Degenhardt, A. Kling, A. Bethge, J. Orf, L. Kärger, R. Zimmermann, K. Rohwer, and A. Calvi. Investigations on imperfection sensitivity and deduction of improved knock-down factors for unstiffened CFRP cylindrical shells. *Composite Structures* 92, (2010) 1939–1946.

[12] J. Arbocz. The imperfection data bank, a mean to obtain realistic buckling loads. In Buckling of shells, 535–567. Springer, 1982.

[13] Simula. Abaqus6.14 GUI toolkit user's guide .

[14] M. Kashfuddoja, R. Prasath, and M. Ramji. Study on experimental characterization of carbon fiber reinforced polymer panel using digital image correlation: A sensitivity analysis. *Optics and Lasers in Engineering* 62, (2014) 17–30.

[15] E. Riks. An incremental approach to the solution of snapping and buckling problems. *International Journal of Solids and Structures* 15.

[16] C. solutions. VIC - 3D reference manual .